Supporting Information

Multiply Intercalator-Substituted Cu(II) Cyclen Complexes as DNA Condensers and DNA/RNA Synthesis Inhibitors

Jan Hormann, Jaroslav Malina, Oliver Lemke, Max J. Hülsey, Stefanie Wedepohl, Jan Potthoff, Claudia Schmidt, Ingo Ott, Bettina G. Keller, Viktor Brabec, and Nora Kulak*

S-1 Synthesis and methods

S-1.1 Preparation of ligands and complexes

Cyclen (**L1**) was provided by Dr. Kai Licha (FU Berlin). 2-(Bromomethyl)anthraquinone, 2-((1,4,7,10-tetraazacyclododecane-1-yl)methyl)anthraquinone (**L2**), 1,4,7,10-tetraazabicyclo[8.2.2]tetradecane-11,12-dione (cyclenoxamide) and 1,7-bis(*tert*-butyloxycarbonyl)-1,4,7,10-tetraazacyclododecane were prepared according to published methods.[1–4]

*Synthesis of [Cu**L1**(NO$_3$)$_2$] and [Zn**L1**(NO$_3$)$_2$]*
The ligand **L1** (0.175 g; 1.02 mmol) and 1.5 equivalents of the corresponding metal source (copper(II) nitrate trihydrate/zinc(II) nitrate hexahydrate) were dissolved in methanol (5 mL). This solution was heated to reflux for 15 min. The formed precipitate was filtered off, washed with cold methanol and dried *in vacuo*.
[Cu**L1**(NO$_3$)$_2$] was obtained as blue needles (0.246 g; 0.69 mmol; 67%). EA (%): Calcd for $C_8H_{20}N_6O_6Cu$ C, 26.70; N, 23.36; H, 5.60. Found C, 26.91; N, 23.06; H, 5.67. ESI-MS: Calcd for [Cu(II) **L1** - H]$^+$ 234.0900, found 234.0909.
[Zn**L1**(NO$_3$)$_2$] was obtained as a white powder (0.259 g; 0.72 mmol; 71%). EA (%): Calcd for $C_8H_{20}N_6O_6Zn$ C, 26.71; N, 22.69; H, 5.57. Found C, 26.71; N, 22.69; H, 5.39. ESI-MS: Calcd for [Zn(II) **L1** + Cl]$^+$ 271.0662, found 271.0675.

*Synthesis of [Cu**L2**(NO$_3$)$_2$]*
The ligand **L2** (0.157 g; 0.40 mmol) was dissolved in chloroform (3 mL), and the solution was heated to reflux. 1.5 equivalents of copper(II) nitrate trihydrate were dissolved in methanol (3 mL) and added to the solution of the ligand. The obtained solution was heated to reflux for another 15 min. The formed precipitate was filtered off, washed with cold methanol and dried i*n vacuo*.
[Cu**L2**(NO$_3$)$_2$] was obtained as a blue solid (0.162 g; 0.28 mmol; 70%). EA (%): Calcd for $C_{23}H_{28}N_6O_8Cu \times 3\ H_2O$ C, 43.57; N, 13.25; H, 5.40. Found C, 43.81; N, 13.03; H, 5.20. ESI-MS: Calcd for [Cu(II) **L2** - H]$^+$ 454.1430, found 454.1438.

*Synthesis of [Zn**L2**(NO$_3$)$_2$]*
The ligand **L2** (0.091 g; 0.23 mmol) was dissolved in chloroform (2 mL), and the solution was heated to reflux. 1.5 equivalents of zinc(II) nitrate hexahydrate were dissolved in methanol (2 mL) and added to the solution of the ligand. The obtained solution was heated to reflux for another 15 min. The formed precipitate was filtered off, washed with ice-cold methanol and dried *in vacuo*.
[Zn**L2**(NO$_3$)$_2$] was obtained as a pale powder (0.090 g; 0.16 mmol; 67%). EA (%): Calcd for $C_{23}H_{28}N_6O_8Zn \times 1\ H_2O \times 0.5\ CH_3OH$ C, 45.83; N, 13.64; H, 5.24. Found C, 45.64; N, 13.68; H, 5.13. ESI-MS: Calcd for [Zn(II) **L2** + Cl]$^+$ 491.1187, found 491.1203.

*Synthesis of **L3** (1,4-Bis-((2-anthraquinonyl)methyl)-cyclen)*
Cyclenoxamide (0.359 g; 1.59 mmol) in abs. DMF (60 mL) was treated with 2-(bromomethyl)anthraquinone (1.056 g; 3.51 mmol) and sodium carbonate (0.920 g; 8.68 mmol). The resulting reaction mixture was stirred for three days at 65 °C and then the solvent was removed under reduced pressure. The crude product was absorbed on silica and purified by column chromatography on silica ($CHCl_3$/isopropylamine; 10/1; R_f 0.6). The so obtained disubstitued cyclenoxamide was suspended in hydrochloric acid (25%; 20 mL) and refluxed for 16 h. After the slurry was diluted to 300 mL by adding

water, the pH value was adjusted to 14 (KOH) and it was extracted three times with chloroform (50 mL). After the combined organic phases were dried over sodium sulfate and the solvent was removed under reduced pressure, the deprotected product **L3** was obtained as a yellow solid (0.309 g; 0.50 mmol; 32%). ^{1}H NMR ($CDCl_3$, 400 MHz) δ: 8.19 (ddd, 4 H, J = 9.4, 4.2 and 2.7 Hz, Ar-H^{25,28,41,44}), 8.13 (d, 2 H, J = 1.8 Hz, Ar-H^{16,32}), 8.08 (d, 2 H, J = 7.9 Hz, Ar-H^{19,35}), 7.75-7.70 (m, 6 H, Ar-H^{20,26,27,36,42,43}), 3.56 (s, 4 H, $CH_2^{13,14}$), 2.85 (s, 4 H, $CH_2^{9,10}$), 2.83-2.81 (m, 4 H, $CH_2^{8,11}$), 2.64 (s, 4 H, $CH_2^{5,6}$), 2.61-2.54 (m, 4 H, $CH_2^{7,12}$) ppm. ^{13}C NMR ($CDCl_3$, 124 MHz) δ: 182.69 (Ar-C^{21,37}), 182.28 (Ar-C^{24,40}), 146.11 (Ar-C^{15,31}), 134.30 (Ar-C^{20,36}), 133.75 (Ar-C$^{26,42\ o.\ 27,43}$), 133.69 (Ar-C$^{26,42\ o.\ 27,43}$), 133.18 (Ar-C$^{22,38\ o.\ 23,39}$), 133.16 (Ar-C$^{22,38\ o.\ 23,39}$), 132.94 (Ar-C^{18,34}), 132.02 (Ar-C^{17,33}), 127.23 (Ar-C^{19,35}), 127.08 (Ar-C^{16,32}), 126.86 (Ar-C$^{25,41\ o.\ 26,44}$), 126.81 (Ar-C$^{25,41\ o.\ 26,44}$), 57.85 ($C^{13,14}$), 52.62 ($C^{7,12}$), 50.70 ($C^{5,6}$), 46.88 ($C^{9,10}$), 45.00 ($C^{8,11}$) ppm. ESI-MS: Calcd for $[C_{38}H_{36}N_4O_4 + H]^+$ 613.2815, found 613.3143.

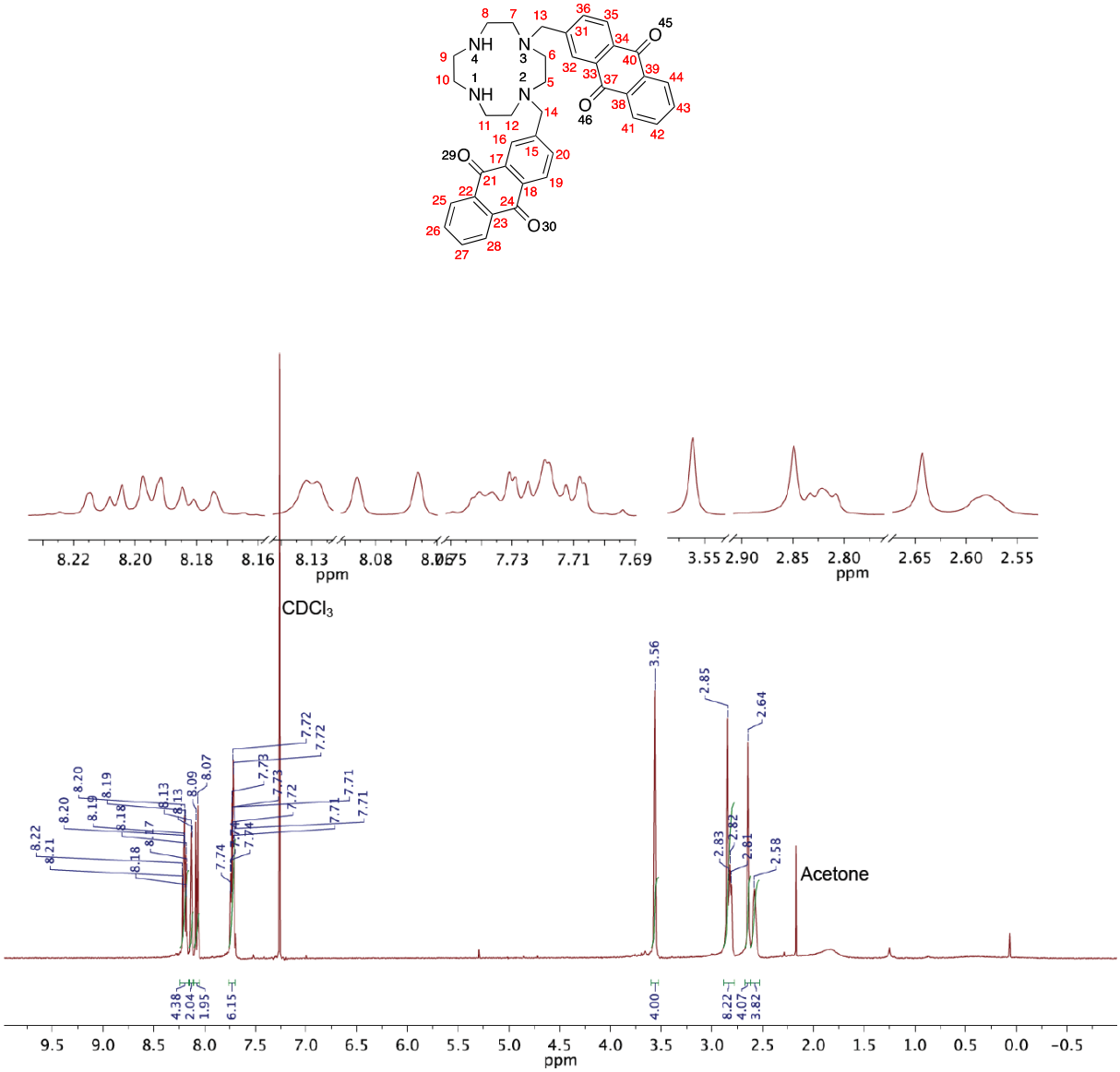

Figure S-1.1 ^{1}H NMR spectrum (400 MHz) of **L3** in $CDCl_3$.

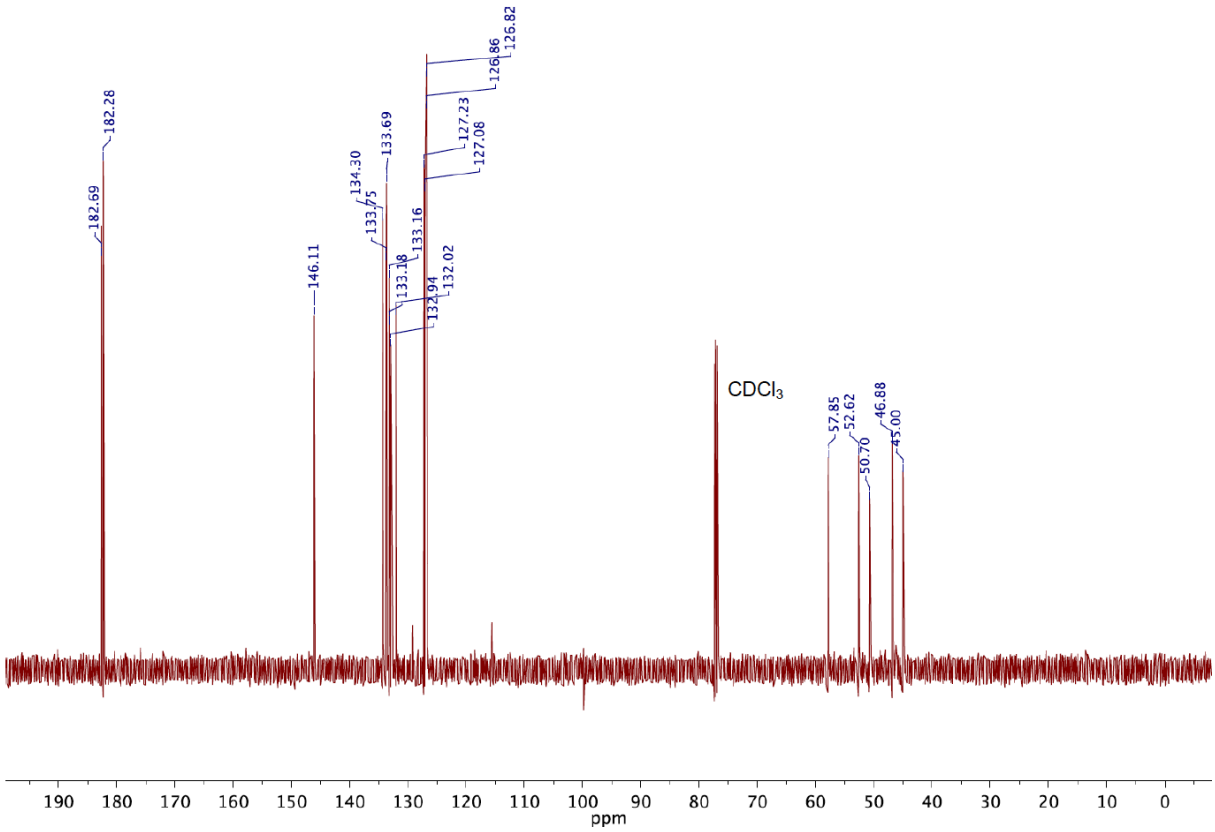

Figure S-1.2 ^{13}C NMR spectrum (124 MHz) of **L3** in $CDCl_3$.

*Synthesis of [Cu**L3**(NO$_3$)$_2$]*

The ligand **L3** (0.310 g; 0.51 mmol) was dissolved in a mixture of chloroform (5 mL) and methanol (5 mL), and the solution was heated to reflux. 1.5 equivalents of copper(II) nitrate trihydrate were dissolved in methanol (5 mL) and added to the solution of the ligand. The obtained solution was heated to reflux for another 15 min. The formed precipitate was filtered off, washed with cold methanol and dried *in vacuo*.

[Cu**L3**(NO$_3$)$_2$] was obtained as a blue powder (0.258 g; 0.32 mmol; 63%). EA (%) Calcd for [Cu**L3**(NO$_3$)$_2$] × 2 H$_2$O: C, 54.53; N, 10.05; H, 4.82. Found C, 54.53; N, 9.85; H, 4.96. ESI-MS: Calcd for [Cu(II) **L3** - H]$^+$ 674.1960, found 674.1975.

*Synthesis of [Zn**L3**(NO$_3$)$_2$]*

The ligand **L3** (0.156 g; 0.25 mmol) was dissolved in chloroform (3 mL), and the solution was heated to reflux. 1.5 equivalents of zinc(II) nitrate hexahydrate were dissolved in methanol (2 mL) and added to the solution of the ligand. The obtained solution was heated to reflux for another 15 min. The formed precipitate was filtered off, washed with ice-cold methanol and dried *in vacuo*.

[Zn**L3**(NO$_3$)$_2$] was obtained as a white powder (0.172 g; 0.21 mmol; 86%). EA (%): Calcd for [Zn**L3**(NO$_3$)$_2$] × 1 H$_2$O C, 55.65; N, 10.25; H, 4.67. Found C, 55.62; N, 10.02; H, 4.73. ESI-MS: Calcd for [Cu(II) **L3** + Cl]$^+$ 711.1711, found 711.1796.

*Synthesis of **L4** (1,7-Bis-((2-anthraquinonyl)methyl)-cyclen)*

1,7-Bis(*tert*-butyloxycarbonyl)-1,4,7,10-tetraazacyclododecane (0.368 g; 0.99 mmol) in abs. acetonitrile (30 mL) was treated with sodium carbonate (0.482 g; 4.55 mmol) and heated to reflux for 30 min. Then a solution of 2-(bromomethyl)anthraquinone (0.549 g; 1.82 mmol) in abs. DMF (15 mL) was added dropwise and after complete addition the reaction mixture was heated to reflux for 19 h. After filtration, the solvent was removed

under reduced pressure and the resulting residue was purified by column chromatography on silica (chloroform; R_f 0.13). The diprotected macrocycle was suspended in hydrochloric acid (25%; 10 mL) and heated to reflux for 3 h. The reaction mixture was diluted to 200 mL by adding water, the pH value was adjusted to 14 (KOH) and the aqueous phase was extracted three times with chloroform (100 mL). After the combined organic phases were dried over sodium sulfate and the solvent was removed under reduced pressure, the 1,7-disubtituted macrocycle **L4** was obtained as a yellow solid (0.342 g; 0.56 mmol; 56%). ^{1}H NMR ($CDCl_3$, 700 MHz) δ: 8.35 (s, 2 H, Ar-H^{17,22}), 8.25-8.21 (m, 4 H, Ar-H^{35,37,41,42}), 8.17 (dd, 2 H, J = 7.2 and 1.9 Hz, Ar-H^{20,25}), 7.79 (dd, 2 H, J = 8.1 and 1.8 Hz, Ar-H^{35,39}), 7.78-7.71 (m, 4 H, Ar-H^{21,26,36,40}), 4.12 (s, 4 H, $CH_2^{13,14}$), 2.96 (s, 8 H, $CH_2^{6,7,10,11}$), 2.89-2.87 (m, 8 H, $CH_2^{5,8,9,12}$) ppm. ^{13}C NMR ($CDCl_3$, 176 MHz) δ: 183.26 (Ar-C^{27,31}), 182.73 (Ar-C^{30,34}), 146.47 (Ar-C^{15,16}), 134.38 (Ar-C$^{36,40\ o.\ 37,41}$), 134.37(Ar-C$^{36,40\ o.\ 37,41}$), 134.20(Ar-C$^{35,39\ o.\ 38,42}$), 133.77 (q), 133.58 (q), 133.44 (q), 132.80 (q), 127.91 (Ar-C$^{35,39\ o.\ 38,42}$), 127.35 (Ar-C^{21,26}), 127.26 (Ar-C^{20,25}), 127.16 (Ar-C^{17,22}), 61.14 (C^{13,14}), 52.44 (C^{6,7,10,11}), 47.97 (C^{5,8,9,12}) ppm. ESI-MS: Calcd for [$C_{38}H_{36}N_4O_4$ + H]$^+$ 613.2815, found 613.2826.

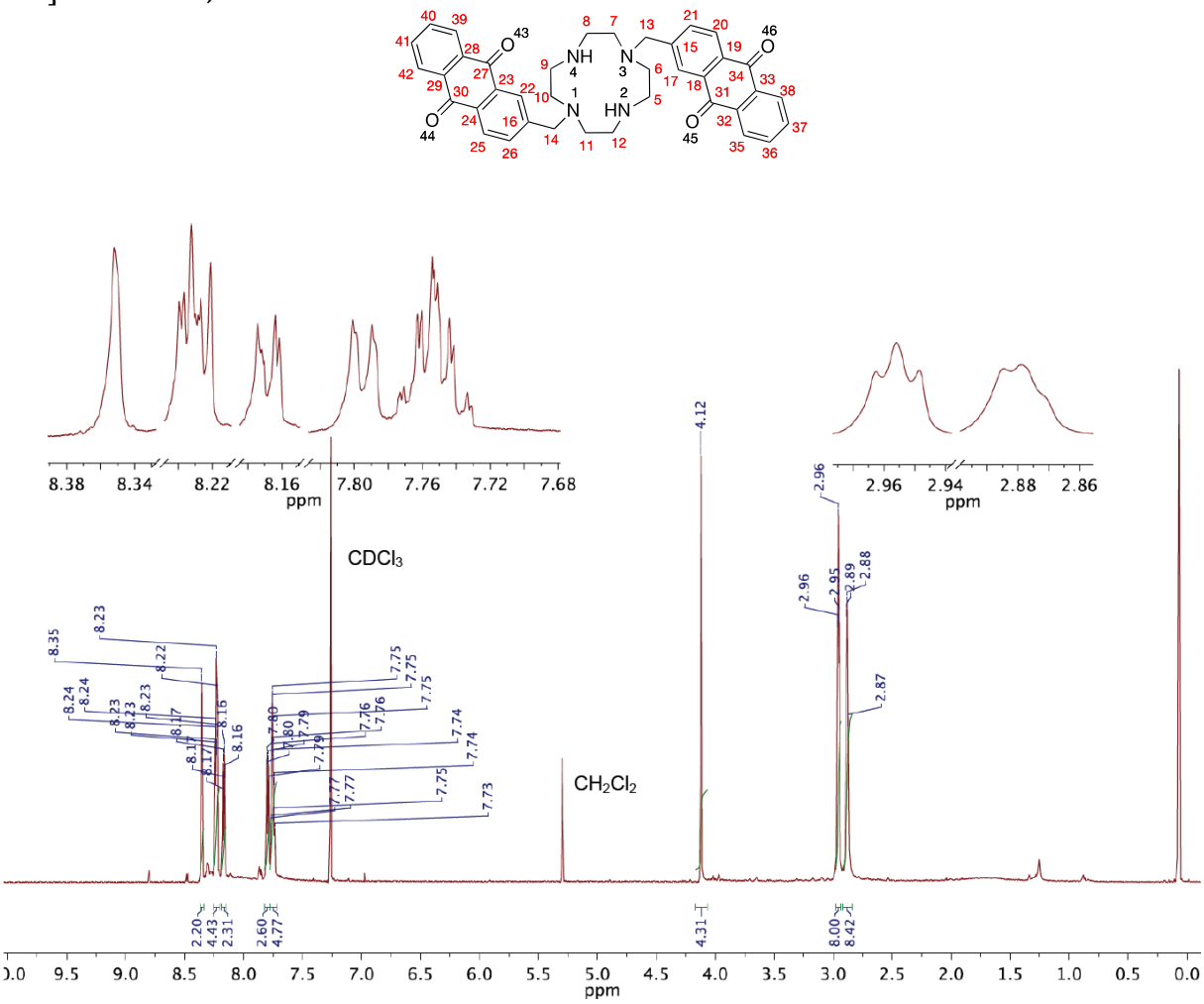

Figure S-1.3 ^{1}H NMR spectrum (700 MHz) of **L4** in $CDCl_3$.

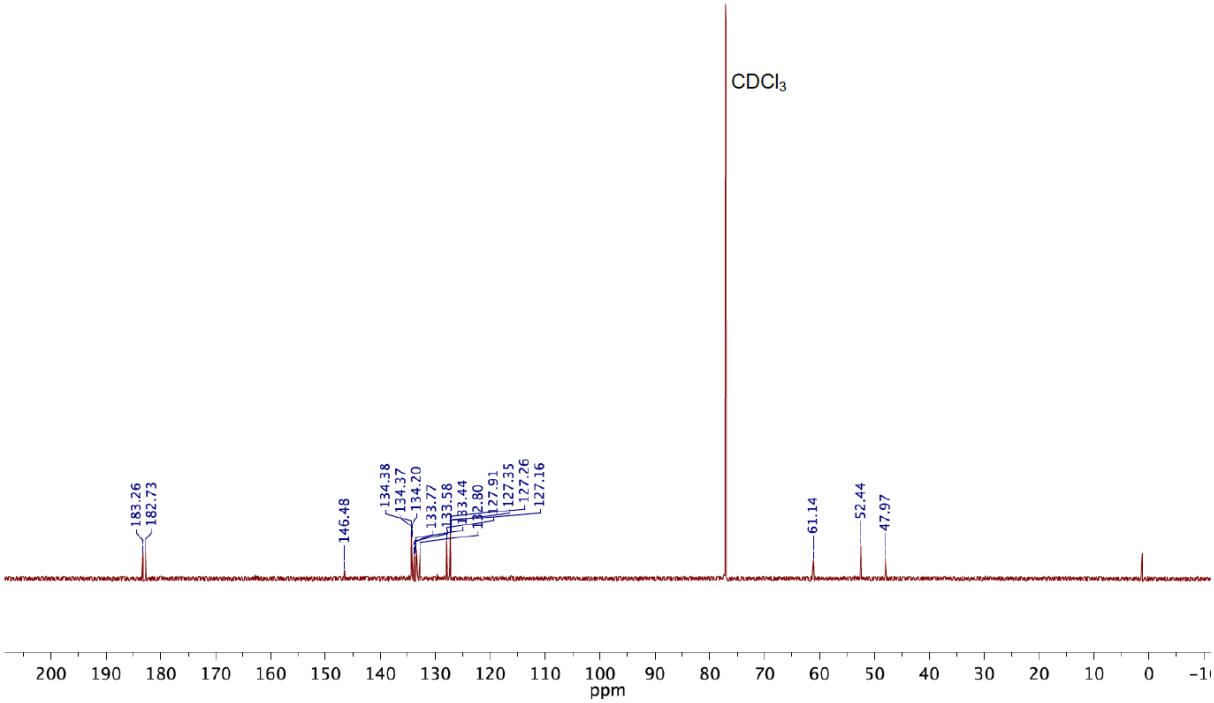

Figure S-1.4 ^{13}C NMR spectrum (176 MHz) of **L4** in $CDCl_3$.

*Synthesis of [Cu**L4**(NO$_3$)$_2$] and [Zn**L4**(NO$_3$)$_2$]*

The ligand **L4** (0.159 g; 0.26 mmol) was dissolved in chloroform (9 mL), and the solution was heated to reflux. 1.5 equivalents of the corresponding metal source (copper(II) nitrate trihydrate/zinc(II) nitrate hexahydrate) were dissolved in methanol (2 mL) and added to the solution of the ligand. The obtained solution was heated to reflux for another 15 min. The formed precipitate was filtered off, washed with ice-cold methanol and dried *in vacuo*.

[Cu**L4**(NO$_3$)$_2$] was obtained as a blue powder (0.136 g; 0.17 mmol; 65%). EA (%) Calcd for [Cu**L4**(NO$_3$)$_2$] × 1.5 CH$_3$OH: C, 55.92; N, 9.91; H, 4.99. Found C, 55.95; N, 9.632; H, 4.80. ESI-MS: Calcd for [Cu(II) **L4** - H]$^+$ 674.1949, found 674.1963.

[Zn**L4**(NO$_3$)$_2$] was obtained as a white powder (0.092 g; 0.12 mmol; 46%). EA (%) Calcd for [Zn**L4**(NO$_3$)$_2$] × 1 CH$_3$OH: C, 56.16; N, 10.07; H, 4.83. Found C, 56.49; N, 9.64; H, 4.82. ESI-MS: Calcd for [Zn(II) **L4** + Cl]$^+$ 711.1711, found 711.1739.

*Synthesis of **L5** (1,4,7-Tris-((2-anthraquinonyl)methyl)-cyclen)*

Over the course of 70 min a solution of 2-bromomethylanthraquinone (2.350 g; 7.80 mmol) in absolute chloroform (70 mL) was added dropwise to a solution of cyclen (0.383 g; 2.22 mmol) and triethylamine (2 mL) in chloroform (40 mL). The reaction mixture was allowed to stay over-night at room temperature, washed with water (3 x 50 mL) and then dried over sodium sulfate. The solvent was removed under reduced pressure and the orange colored residue was purified *via* column chromatography on silica (chloroform/triethylamine; 100/1; R_f 0.05) to yield **L5** (0.673 g; 0.81 mmol; 36%) as an orange solid. ^{1}H NMR ($CDCl_3$, 700 MHz) δ: 8.20-8.17 (m, 4 H, Ar-H^{21,33,49,52}), 8.15-8.09 (m, 6 H, Ar-H^{27,29,42,44,58,60}), 7.88-7.81 (m, 4 H, Ar-H^{17,18,36,37}), 7.72 (d, 1 H, J = 7.3 Hz, Ar-H^{53}), 7.70-7.63 (m, 6 H, Ar-H^{26,28,43,45,59,61}), 3.67 (s, 4 H, CH$_2^{14,15}$), 3.33 (s, 2 H, CH$_2^{13}$), 2.82 (s, 4 H, CH$_2^{10,11}$), 2.70 (s, 4 H, CH$_2^{5,8/6,7}$), 2.64 (s, 4 H, CH$_2^{9,12}$), 2.54 (s, 4 H, CH$_2^{5,8/6,7}$) ppm. ^{13}C NMR ($CDCl_3$, 176 MHz) δ: 183.17 (Ar-C^{25,38}), 182.92 (Ar-C^{54}), 182.70 (Ar-C^{22,41}), 182.46 (Ar-C^{57}), 146.47 (Ar-C^{48}), 146.11 (Ar-C^{16,32}), 135.00 (Ar-C), 134.08

(Ar-C), 133.96 (Ar-C), 133.94 (Ar-C), 133.82 (Ar-C), 133.55 (*q*, Ar-C), 133.52 (*q*, Ar-C), 133.51 (*q*, Ar-C), 133.46 (*q*, Ar-C), 133.34 (*q*, Ar-C), 133.05 (*q*, Ar-C), 132.44 (*q*, Ar-C), 132.09 (*q*, Ar-C), 127.74 (Ar-C), 127.50 (Ar-C), 127.38 (Ar-C), 127.23 (Ar-C), 127.11 (Ar-C), 127.10 (Ar-C), 126.74 (Ar-C^{49}), 59.68 ($C^{14,15}$), 57.05 (C^{13}), 52.59 ($C^{5,8/6,7}$), 52.21 ($C^{5,8/6,7}$), 50.13 ($C^{9,12}$), 46.92 ($C^{10,11}$) ppm. EA (%): Calcd for $C_{53}H_{45}N_4O_6$ × 1 $CHCl_3$ × 1 CH_3OH C, 65.98; N, 5.47; H, 5.61. Found C, 65.73; N, 5.43; H, 5.37. ESI-MS: Calcd for $[C_{53}H_{44}N_4O_6 + H]^+$ 833.3334, found 833.3310.

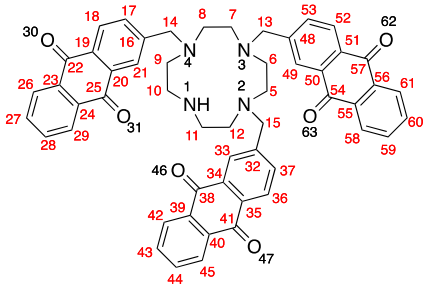

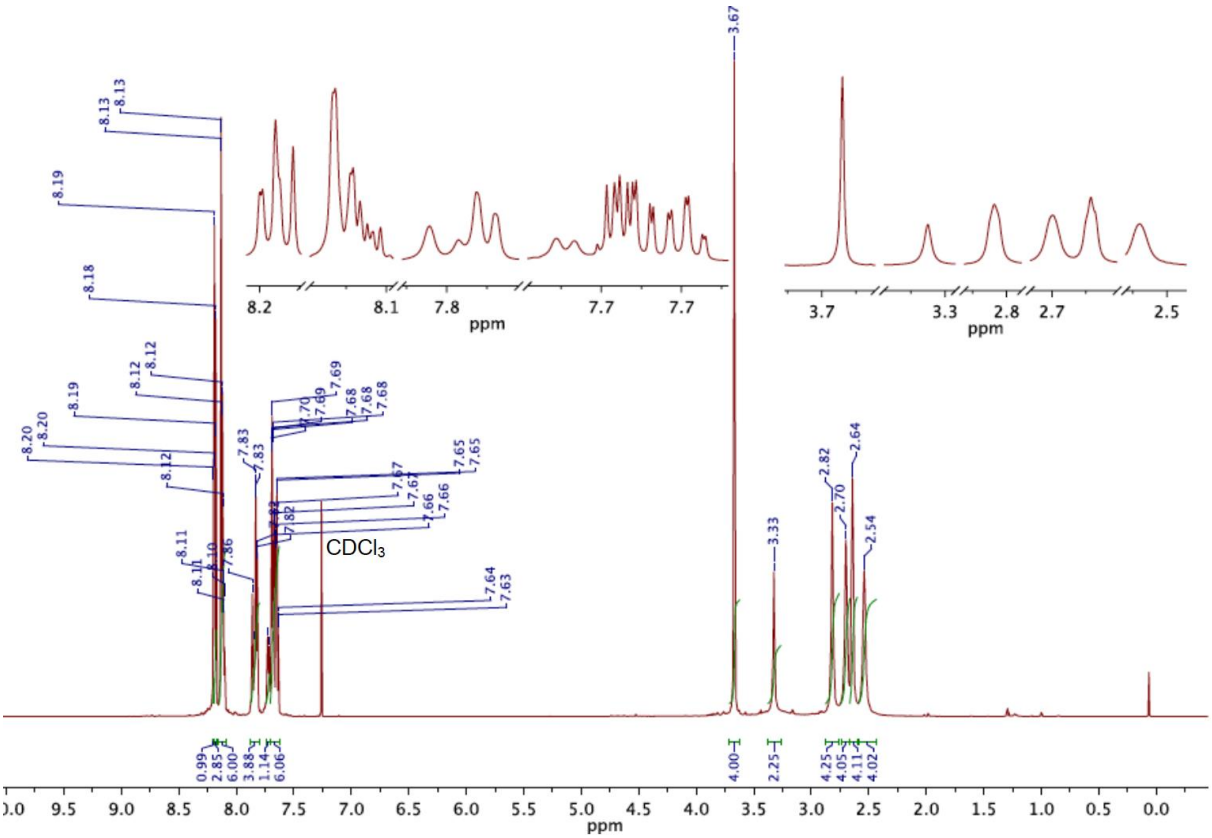

Figure S-1.5 ^{1}H NMR spectrum (700 MHz) of **L5** in $CDCl_3$.

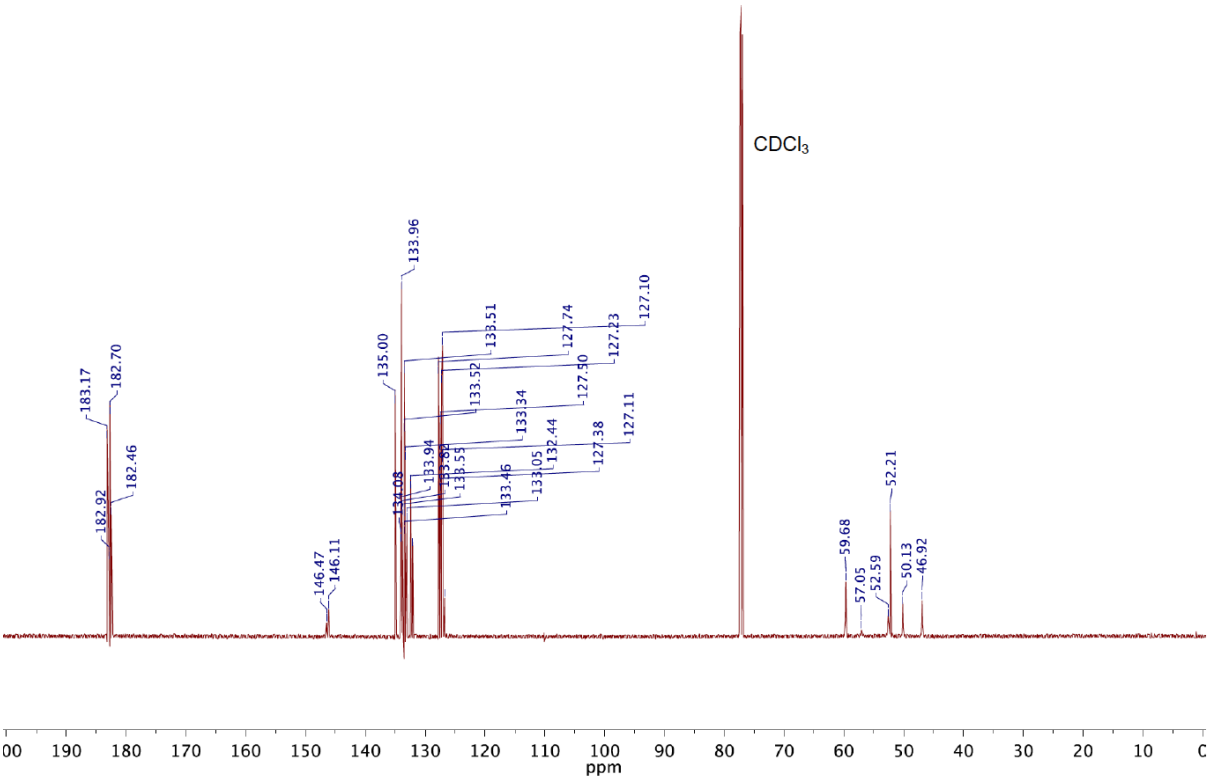

Figure S-1.6 ^{13}C NMR spectrum (176 MHz) of **L5** in $CDCl_3$.

*Synthesis of [Cu**L5**$(NO_3)_2$] and [Zn**L5**$(NO_3)_2$]*

The ligand **L5** (0.203 g; 0.24 mmol) was dissolved in chloroform (2 mL), and the solution was heated to reflux. 1.5 equivalents of the corresponding metal source (copper(II) nitrate trihydrate/zinc(II) nitrate hexahydrate) were dissolved in methanol (2 mL) and added to the solution of the ligand. The obtained solution was heated to reflux for another 15 min. The formed precipitate was filtered off, washed with cold methanol and dried *in vacuo*.

[Cu**L5**$(NO_3)_2$] was obtained as a blue powder (0.206 g; 0.20 mmol; 83%). EA (%) Calcd for [Cu**L5**$(NO_3)_2$] × 3 H_2O: C, 59.14; N, 7.81; H, 4.68. Found C, 59.32; N, 7.97; H, 4.71. ESI-MS: Calcd for [Cu(II) **L5** - H]$^+$ 894.2479, found 894.2473.

[Zn**L5**$(NO_3)_2$] was obtained as a white powder (0.196 g; 0.19 mmol; 79%). EA (%) Calcd for [Zn**L5**$(NO_3)_2$] × 3.5 H_2O: C, 58.75; N, 7.76; H, 4.74. Found C, 58.78; N, 8.03; H, 4.67. ESI-MS: Calcd for [Zn(II) **L5** + Cl]$^+$ 931.2241, found 931.2255.

S-1.2 Methods

X-Ray: Single crystals of $C_{23}H_{28}CuN_6O_8$ ([Cu**L2**(NO_3)]NO_3) were obtained by slow diffusion of diethyl ether into a saturated methanolic complex solution. A suitable crystal (0.31 × 0.16 × 0.15 mm) was selected and its structure was determined on a Bruker APEX-II CCD diffractometer. The crystal was kept at 100.06 K during data collection. Using Olex2[5] the structure was solved with the olex2.solve[6] structure solution program using Charge Flipping and refined with the ShelXL[7] refinement package using Least Squares minimization.

UV melting: Melting curves of buffered (Tris-HCl; 50 mM; pH 7.4) CT-DNA (100 µM) were measured using a Varian Cary 100 Bio UV/Vis spectrophotometer in the presence of ligands, copper or zinc complexes (2.5 µM) at 260 nm (heating rate 0.5 °C/min). The

experiments were carried out simultaneously in four 1 cm path length Helma cuvettes with 1 mL sample volume. Melting temperatures were calculated using the thermal heating program by applying a first derivative calculation. For visualization melting curves were normalized.

Ethidium bromide (EB) displacement: The fluorescence emission spectra of intercalated ethidium bromide were collected using a Varian Cary Eclipse fluorescence spectrophotometer. A solution of CT-DNA or of homopolymers poly(dG)×poly(dC) and poly(dA)×poly(dT) (20 μM), EB (5 μM) and Tris-HCl (10 mM, pH 7.4) in a 1 cm fluorescence cuvette was treated with increasing concentrations of the corresponding complex. In order to get a stable I_o value for intercalated EB, an incubation time of 5 min ((poly(dG)×poly(dC)) and 4 h (poly(dA)×poly(dT)), respectively, was inserted. After each addition of the complex the fluorescence spectrum between 530 and 750 nm was collected. The excitation wavelength was 518 nm. The voltage of the photomultiplier was adjusted between 900 and 980 V in order to keep the emission of the CT-DNA-EB system between 800 and 1000 a.u.

Flow linear dichroism (LD): Flow LD spectra were collected by using a flow Couette cell in a Jasco J-720 spectropolarimeter adapted for LD measurements. Long molecules, such as DNA (minimum length of ~250 bp), can be orientated in a flow Couette cell. The flow cell consists of a fixed outer cylinder and a rotating solid quartz inner cylinder, separated by a gap of 0.5 mm, giving a total path length of 1 mm. LD spectra of CT-DNA, poly(dG)xpoly(dC) and poly(dA)xpoly(dT) at a concentration of 2×10^{-4} M were recorded at 25 °C in 10 mM Tris-HCl (pH 7.4).[8,9]

Total intensity light scattering: Light scattering experiments were performed using similar conditions to those described by Vijayanathan *et al.*[10] The experiments were carried out in 10 mM cacodylate buffer (pH 7.2). All buffers and stock solutions of copper complexes were filtered through 0.2 μm filters before use to avoid interference from dust particles. A 1.5 μM solution of CT-DNA was prepared in a 1 cm quartz cuvette in a total volume of 2.5 mL. Small volumes (<10 μL) of copper complexes were added to the CT-DNA solution to obtain the desired concentration and the solution was thoroughly mixed by pipetting. The mixture was kept undisturbed for 5 min at room temperature. Total intensity light scattering was measured by using Varian Cary Eclipse spectrofluorophotometer. The excitation and emission wavelengths were set to 305 nm, the excitation and emission slit widths were 5 nm, and the integration time was set to 5 s. The scattered light was measured at 90° angle with respect to the incident beam.

Gel retardation: pBR322 plasmid DNA (0.025 μg μL^{-1}) was incubated with the Cu(II) complexes (2.5-50 μM) for 30 min at 37 °C in Tris-HCl buffer (50 mM, pH 7.4). The total reaction volume was adjusted to 8 μL by adding deionized water (Millipore system). For analysis, 1.5 μL of loading buffer (containing 3.7 mM bromophenol blue and 1.2 M saccharose in deionized water) was added to the incubation solution and loaded onto an agarose (SeaKem LE, Lonza) gel (1% in 0.5X Tris-borate-EDTA (TBE) buffer, Fisher Scientific) containing EB (0.2 μg mL^{-1}, Fisher Scientific). Electrophoresis was carried out at 40 V for 2 h with an electrophoresis unit (Carl Roth; power supply: consort EV243) in 0.5X TBE buffer. Bands were visualized by UV light and photographed by using a gel documentation system (GelDoc, Bio-Rad). To make sure that results were reliable the experiments were conducted three times each.

AFM imaging: The plasmid pSP73 (2464 bp) was linearized by digestion with *Nde* I restriction endonuclease and purified using Promega Wizard SV Gel clean-up system. The Cu(II) complexes were dissolved in MilliQ water (Millipore System, Billerica, MA), mixed with DNA (20 ng) in 10 μL to obtain the desired concentration in the buffer containing 4 mM HEPES (pH 7.4), 5 mM KCl and 5 mM $MgCl_2$ and incubated for 5 min at room temperature. A droplet (4 μL) of the mixture was spotted directly onto freshly cleaved mica (SPI, West Chester, PA). After 2 min incubation, the mica was gently rinsed with 1 mL of MilliQ water and immediately blown dry with compressed air. Imaging was performed using a MultiMode 8 atomic force microscope (Bruker, Santa Barbara, CA). Scanning was carried out in ScanAsyst mode in air using ScanAsyst-Air probes from Bruker (Camarillo, CA, USA).

PCR: A 279 bp insert from linearized pBR322 plasmid DNA was amplified via PCR using the oligonucleotide primers GCTGATGAGCTTTACCGCAGCTGCCTCGC and CGCATCTGTGCGGTATTTCACACCGC. About 1 ng of the plasmid was incubated with 0.1 μM of each primer and the Qiagen Taq PCR Master Mix Kit (2.5 U Taq DNA Polymerase; 1X Qiagen PCR buffer; 200 μM dNTP). The incubations were performed under addition of various concentrations of the compounds of interest. The overall incubation volume was 25 μL. To make sure that the conditions in each sample were the same, 1% DMSO and 1X PBS buffer were added. After 25 PCR cycles the reaction products were analyzed by agarose gel electrophoresis (1% in TBE including 0.1% EB; 40 V; 30 min).

DNA transcriptional activity: Transcription and detection of RNA products was performed according to the procedure described by Luckel *et al*.[11] This assay is based on using of a fluorescent analog of UTP (UTP γ-AmNS) as one of the nucleotide substrates. Incorporation of UMP in RNA leads to the release of γ-AmNS, which exhibits higher intrinsic fluorescence than UTP γ-AmNS. pBR322 plasmid DNA at the concentration of 3×10^{-5} M (per nucleotide) was used as a template. Transcription was carried out in 28 μL reaction volume containing 10 mM Tris-HCl buffer (pH 7.6), 100 mM KCl, 5 mM $MgCl_2$, 0.1 mM ATP, CTP and GTP, 0.01 mM UTP γ-AmNS, 2 mM dithiothreitol, and various concentrations of Cu(II) complexes. After 10 min of pre-incubation at room temperature, one unit of *E. coli* RNA polymerase holoenzyme was added and transcription was performed for 2 h at 37 °C. The reaction was stopped by addition of 42 μL of 50 mM EDTA and transcription products were detected by measuring the sample fluorescence intensity at 465 nm using a Varian Cary Eclipse fluorescence spectrophotometer. The excitation wavelength was set to 330 nm, the excitation and emission slit widths were 5 nm, and the integration time was set to 5 s.

Cell culture: A549 (lung epithelium carcinoma) and NHDF (normal human dermal fibroblast) cells were routinely maintained in DMEM with GlutaMAX (Dulbecco's minimal essential medium, Thermo Fisher Scientific), 10% FBS (FBS Superior, Biochrom AG) and 1% penicillin/streptomycin (Thermo Fisher Scientific) at 37 °C and 5% CO_2.

Cell viability assays: For MTT assay, 1×10^5 cells/mL were seeded into 96 well plates and incubated over-night at 37 °C and 5% CO_2. The next day, medium was replaced with 100 μL per well fresh medium containing dilutions of the test compounds (in duplicates). After 48 h of incubation, 10 μL MTT (3-(4,5-dimethylthiazol-2-yl)-2,5-diphenyltetrazolium bromide, 5 mg/mL stock solution in PBS, Sigma) in 100 μL fresh medium/well was added and incubated for 4 h at 37 °C and 5% CO_2. The supernatant was then discarded and formazan crystals were solubilized in 100 μL/well isopropanol

with 0.04 M HCl. Absorbance was read in a microplate reader (Tecan Infinite M200Pro) at 570 nm. Assays were repeated at least three times independently.
Relative cell viabilities were calculated by dividing the average absorbance values of duplicates by the absorbance value of untreated cells. The average of at least three experiments were then plotted with their SEM against concentration. IC_{50} values and 95% CI were calculated from nonlinear dose-response curves (log inhibitor vs. normalized response – variable slope) fitted in GraphPadPrism software.
In addition, for selected samples the number of intact cells was determined by flow cytometry. For this, 60000 NHDF cells were seeded into 24 well plates and grown over night. The next day, medium was replaced with 600 µl/well fresh medium containing 500 µM, 0.5 µM or 0.05 µM Cu(II) **L2**, **L4** and **L5**, respectively. After 48 h of incubation, cells were washed, trypsinized and events in a defined volume were counted in a BD Accuri™ C6 flow cytometer. Cell debris was excluded by gating the main population of untreated cells in a forward scatter versus sideward scatter plot.

Cellular uptake studies: A549 cells were seeded into sixteen 25 cm^2 cell culture flasks. When the bottles contained roughly at least two million cells, the cells were incubated with the complexes at a concentration of 1.5 µM. As triplicates were used, six flasks were incubated with Cu(II) **L1**, six flasks were incubated with Cu(II) **L4** and four flasks were untreated and used as controls. After 6 h, half of the incubated cells were washed with PBS, trypsinized and centrifuged for 4 min at 140 × g (three flasks incubated with Cu(II) **L1**, three flasks incubated with Cu(II) **L4** and two flasks without treatment) and then after 24 h the remaining cells were harvested by trypsinization as before. The harvested cells were centrifuged in Eppendorf tubes, the supernatant was removed and the pellets were frozen.
For metal and protein quantification, the pellets were resuspended in demineralized water (250 µL) and lysed for 30 min by ultrasonication. The protein content of lysates was determined by the Bradford method, and the copper content was determined with a contrAA 700 high-resolution continuum-source atomic absorption spectrometer (Analytik Jena AG). Pure samples of the respective copper complex were used to prepare standards (stock solutions were prepared with DMSO) and calibration was done in a matrix-matched manner (meaning all samples and standards were adjusted to the same cellular protein concentration of 1.0 mg/mL by dilution with distilled water if necessary).
Triton-X 100 (1%, 10 µL) as well as nitric acid (13%, 10 µL), were added to each standard sample (100 µL). Samples were injected (15 µL) into a coated standard graphite tube (Analytik Jena AG) and thermally processed as in the table below. Copper was quantified at a wavelength of 324.7540 nm. The mean integrated absorbance of double injections was used throughout the measurements.

Table S-1 Temperature program for AAS measurements.

Steps	Temperature [°C]	Ramp [°C/s]	Hold [s]	Argon purge
Drying	80	6	20	max
Drying	90	3	20	max
Drying	110	5	10	max
Pyrolysis	350	50	20	max
Pyrolysis	1100	300	10	max
Gas adaption	1100	0	5	stop
Atomize	2000	1500	4	stop
Cleaning	2450	500	4	max

Molecular Modelling: As a starting structure for the molecular modelling the DNA crystal structure with the PDB-ID 440D[12] was used. The ligand structures were generated using the Marvin Suite.[13] Afterwards, the ligands were protonated at pH 7.4 and energy minimized *in vacuo* using Avogadro.[14] As a conformation generator AutoDockTools[15] was applied. An insertion of the ligands into the DNA was performed with PyMol.[16] The ligand-DNA-complex was then energy minimized *in vacuo*, solvated in TIP3P water[17] and again energy minimized using the GROMACS simulation package 5.0.2.[18] For the DNA as well as the metal ion the AMBER94-force field was applied.[19] The force field parameters for the ligands without the metal center were generated using AmberTools 16 and ACPYPE.[20,21]

S-2 X-ray structure determination

Table S-2.1 Crystal data and structure refinement for [Cu**L2**(NO_3)]NO_3 (CCDC 1532772).

Empirical formula	$C_{23}H_{28}CuN_6O_8$
Formula weight	580.05
Temperature/K	100.06
Crystal system	triclinic
Space group	P-1
a/Å	10.6533(11)
b/Å	10.7743(11)
c/Å	12.9755(13)
α/°	91.367(5)
β/°	109.066(4)
γ/°	98.645(5)
Volume/Å^3	1387.4(2)
Z	2
ρ_{calc}g/cm^3	1.388
μ/mm^{-1}	0.842
F(000)	602.0
Crystal size/mm^3	0.31 × 0.16 × 0.15
Radiation	MoKα (λ = 0.71073)
2Θ range for data collection/°	4.88 to 52.902
Index ranges	-13 ≤ h ≤ 13, -13 ≤ k ≤ 13, -16 ≤ l ≤ 16
Reflections collected	31525
Independent reflections	5700 [R_{int} = 0.0343, R_{sigma} = 0.0232]
Data/restraints/parameters	5700/0/343
Goodness-of-fit on F^2	1.082
Final R indexes [I>=2σ (I)]	R_1 = 0.0280, wR_2 = 0.0667
Final R indexes [all data]	R_1 = 0.0333, wR_2 = 0.0690
Largest diff. peak/hole / e Å^{-3}	0.42/-0.33

Table S-2.2 Bond lengths for [Cu**L2**(NO_3)]NO_3.

		bond length [Å]			bond length [Å]
Cu1	O31	2.164(1)	C11	C12	1.516(2)
Cu1	N1	2.075(1)	C13	C14	1.513(2)
Cu1	N4	2.015(1)	C14	C15	1.397(2)
Cu1	N7	2.025(1)	C14	C19	1.393(2)
Cu1	N10	2.002(1)	C15	C16	1.386(2)
O28	C23	1.224(2)	C16	C17	1.388(2)
O29	C20	1.228(2)	C17	C18	1.399(2)
O31	N30	1.278(2)	C17	C20	1.488(2)
O32	N30	1.246(2)	C18	C19	1.391(2)
O33	N30	1.237(2)	C18	C23	1.484(2)
N1	C2	1.499(2)	C20	C21	1.484(3)
N1	C12	1.484(2)	C21	C22	1.395(3)
N1	C13	1.497(2)	C21	C24	1.393(2)
N4	C3	1.480(2)	C22	C23	1.486(2)
N4	C5	1.490(2)	C22	C27	1.390(3)
N7	C6	1.472(2)	C24	C25	1.383(3)
N7	C8	1.486(2)	C25	C26	1.383(3)
N10	C9	1.485(2)	C26	C27	1.384(3)
N10	C11	1.481(2)	O35	N34	1.266(2)
C2	C3	1.511(2)	O36	N34	1.250(2)

C5	C6	1.512(3)	O37	N34	1.236(2)
C8	C9	1.514(3)			

Table S-2.3 Bond angles for [Cu**L2**(NO_3)]NO_3.

			bond angle [°]				bond angle [°]
N1	Cu1	O31	104.07(5)	N10	C11	C12	108.96(13)
N4	Cu1	O31	98.05(5)	N1	C12	C11	109.25(13)
N4	Cu1	N1	85.55(5)	N1	C13	C14	114.85(13)
N4	Cu1	N7	86.30(6)	C15	C14	C13	120.18(15)
N7	Cu1	O31	106.35(5)	C19	C14	C13	121.19(14)
N7	Cu1	N1	149.31(6)	C19	C14	C15	118.60(15)
N10	Cu1	O31	112.89(5)	C16	C15	C14	120.61(15)
N10	Cu1	N1	86.88(5)	C15	C16	C17	120.65(15)
N10	Cu1	N4	149.06(6)	C16	C17	C18	119.30(15)
N10	Cu1	N7	85.08(6)	C16	C17	C20	119.70(15)
N30	O31	Cu1	118.87(10)	C18	C17	C20	121.00(15)
C2	N1	Cu1	106.73(9)	C17	C18	C23	120.95(15)
C12	N1	Cu1	100.89(9)	C19	C18	C17	119.77(15)
C12	N1	C2	111.57(12)	C19	C18	C23	119.26(15)
C12	N1	C13	113.05(12)	C18	C19	C14	121.05(15)
C13	N1	Cu1	113.50(9)	O29	C20	C17	120.68(16)
C13	N1	C2	110.62(12)	O29	C20	C21	121.42(16)
C3	N4	Cu1	103.03(10)	C21	C20	C17	117.90(15)
C3	N4	C5	113.79(13)	C22	C21	C20	120.99(15)
C5	N4	Cu1	107.40(10)	C24	C21	C20	119.20(16)
C6	N7	Cu1	104.29(10)	C24	C21	C22	119.80(17)
C6	N7	C8	114.88(14)	C21	C22	C23	121.20(16)
C8	N7	Cu1	108.80(11)	C27	C22	C21	119.52(16)
C9	N10	Cu1	105.13(10)	C27	C22	C23	119.26(17)
C11	N10	Cu1	108.30(10)	O28	C23	C18	120.88(15)
C11	N10	C9	114.11(13)	O28	C23	C22	121.22(16)
O32	N30	O31	119.22(13)	C18	C23	C22	117.90(15)
O33	N30	O31	119.01(14)	C25	C24	C21	120.16(18)
O33	N30	O32	121.76(14)	C24	C25	C26	119.99(17)
N1	C2	C3	110.55(13)	C25	C26	C27	120.26(19)
N4	C3	C2	108.51(13)	C26	C27	C22	120.25(19)
N4	C5	C6	109.44(14)	O36	N34	O35	118.13(14)
N7	C6	C5	107.52(14)	O37	N34	O35	120.97(15)
N7	C8	C9	109.26(13)	O37	N34	O36	120.91(15)
N10	C9	C8	106.70(14)				

S-3 DNA melting

Table S-3 Effect of ligands **L1**–**L5** (2.5 µM) and their Zn(II) (2.5 µM) and Cu(II) complexes (marked in red, 2.5 µM) on the melting temperature of CT-DNA (100 µM, T_m = 82.4 ± 0.2 °C) in Tris-HCl buffer (50 mM, pH 7.4) and 1% DMSO. Despite aggregation of DNA the maximum absorption values for dehybridized DNA (here normed to 1) were similar for all compounds indicating that the DNA concentration was constant under these assay conditions.

	ΔT_m
CT-DNA	0.0 ± 0.2
L1	0.1 ± 0.2
Zn(II) **L1**	-0.4 ± 0.9
Cu(II) **L1**	0.2 ± 0.3
L2	2.8 ± 1.7
Zn(II) **L2**	5.1 ± 1.3
Cu(II) **L2**	6.0 ± 2.8
L3	1.0 ± 0.0
Zn(II) **L3**	1.8 ± 0.3
Cu(II) **L3**	5.0 ± 1.5
L4	1.6 ± 0.5
Zn(II) **L4**	2.6 ± 0.6
Cu(II) **L4**	1.6 ± 0.6
L5	1.4 ± 0.4
Zn(II) **L5**	1.2 ± 0.3
Cu(II) **L5**	1.0 ± 0.1

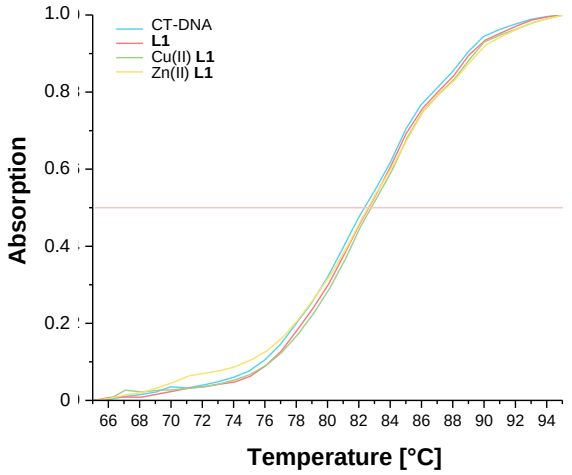

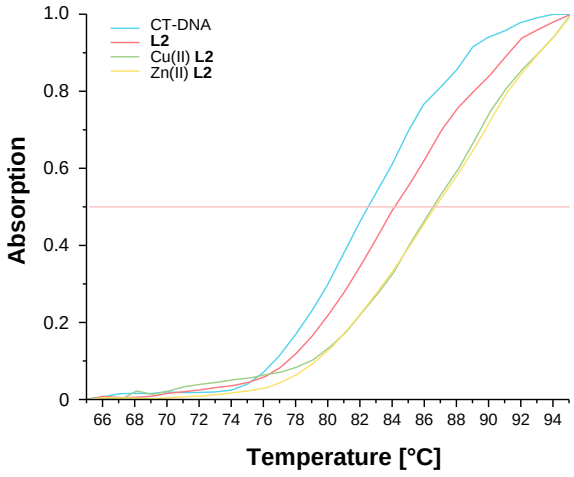

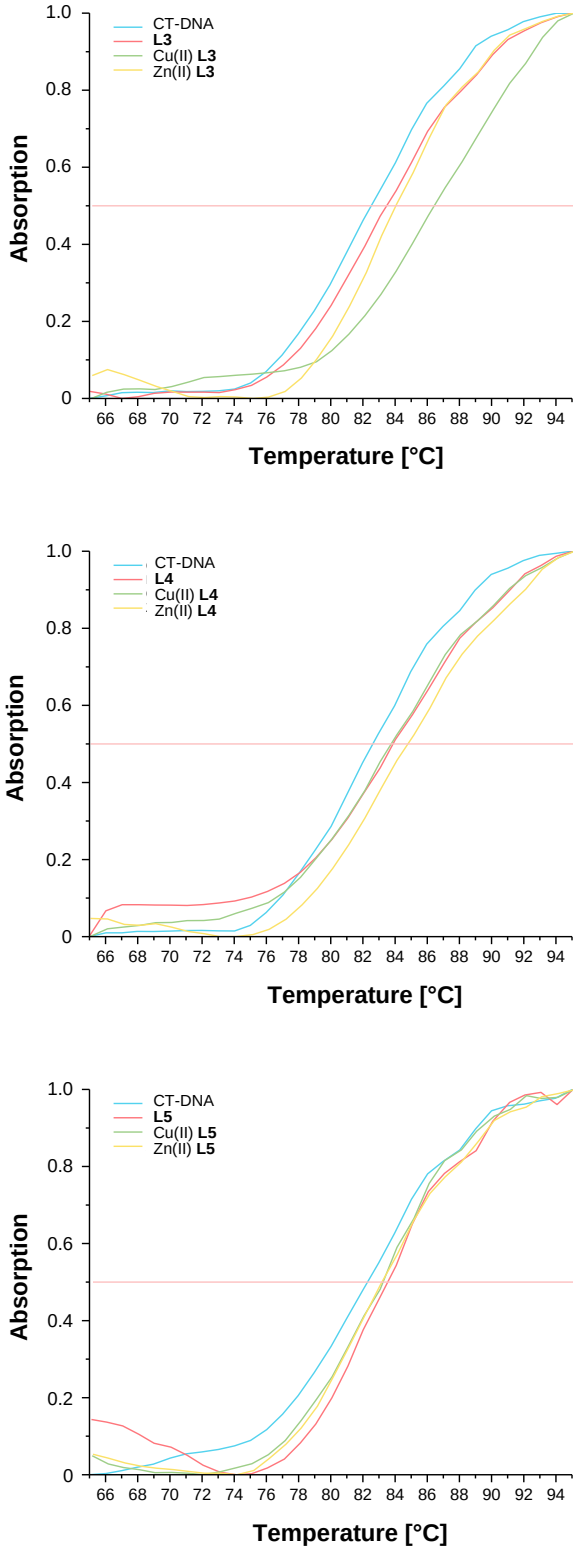

Figure S-3 Representative melting curves of CT-DNA (100 μM) under addition of ligands **L1**–**L5** and their Zn(II) and Cu(II) complexes (2.5 μM), respectively, in Tris-HCl buffer (50 mM, pH 7.4) and 1% DMSO.

S-4 Ethidium bromide displacement

The fluorescence data were evaluated by using the Stern-Volmer equation:

$$\frac{I_0}{I} = 1 + K_{SV}[Q]$$

with I_0 being the original intensity of EB at 605 nm, I the intensity in the presence of the Cu(II) complexes as quenchers and the concentration of the quencher $[Q]$. The Stern-Volmer constant K_{SV} is a measure of the intercalation capacity of an intercalating quencher and it can be obtained by plotting the quotient of I_0 and I against $[Q]$.

For obtaining the apparent binding constants K_{app}, the following formula was applied:

$$K_{EB}[EB] = K_{app}[Q]$$

with K_{EB} being the binding constant for EB towards CT-DNA (1.00×10^7 M^{-1}),[22] poly(dG)×poly(dC) (1.28×10^7 M^{-1})[23] and poly(dA)×poly(dT) DNA (1.85×10^6 M^{-1}),[23,*] the concentration of EB $[EB]$ = 5 µM and $[Q]$ being the concentration of the complexes, at which half of the original fluorescence intensity was quenched.

Table S-4.1 K_{SV} values [M^{-1}] of Cu(II) complexes of ligands **L1** to **L5** determined by the EB displacement assay of CT-DNA and homopolymers poly(G)×poly(C) and poly(A)×poly(T) (20 µM DNA, 5 µM EB) in Tris-HCl buffer (10 mM, pH 7.4).

	K_{SV} [M^{-1}] x 10^6		
	CT-DNA	poly(dG)×poly(dC)	poly(dA)×poly(dT)
Cu(II) **L1**	0.087	0.123	0.054
Cu(II) **L2**	1.451	0.993	0.903
Cu(II) **L3**	0.675	0.196	0.831
Cu(II) **L4**	0.145	0.111	0.223
Cu(II) **L5**	0.079	0.069	0.054

* Baguley *et al.*[23] calculated K_{EB} = 3.5 × 10^6 M^{-1} for CT-DNA under the conditions they used. For this reason, the values for the other two binding constants were adjusted accordingly by multiplying the literature values by 2.85.

Table S-4.2 K_{app} [M^{-1}] values of Cu(II) complexes of ligands **L1** to **L5** determined by the EB displacement assay of CT-DNA and homopolymers poly(G)×poly(C) and poly(A)×poly(T) (20 μM DNA, 5 μM EB) in Tris-HCl buffer (10 mM, pH 7.4). Values for bisintercalation are considered in parentheses.

	K_{app} [M^{-1}] x 10^7		
	CT-DNA	poly(dG)×poly(dC)	poly(dA)×poly(dT)
Cu(II) **L1**	0.435	0.787	0.050
Cu(II) **L2**	7.255	6.355	0.835
Cu(II) **L3**	3.375	1.254	0.769
Cu(II) **L4**	0.725 (1.450)	0.710 (1.420)	0.206 (0.412)
Cu(II) **L5**	0.395 (0.790)	0.442 (0.884)	0.050 (0.100)

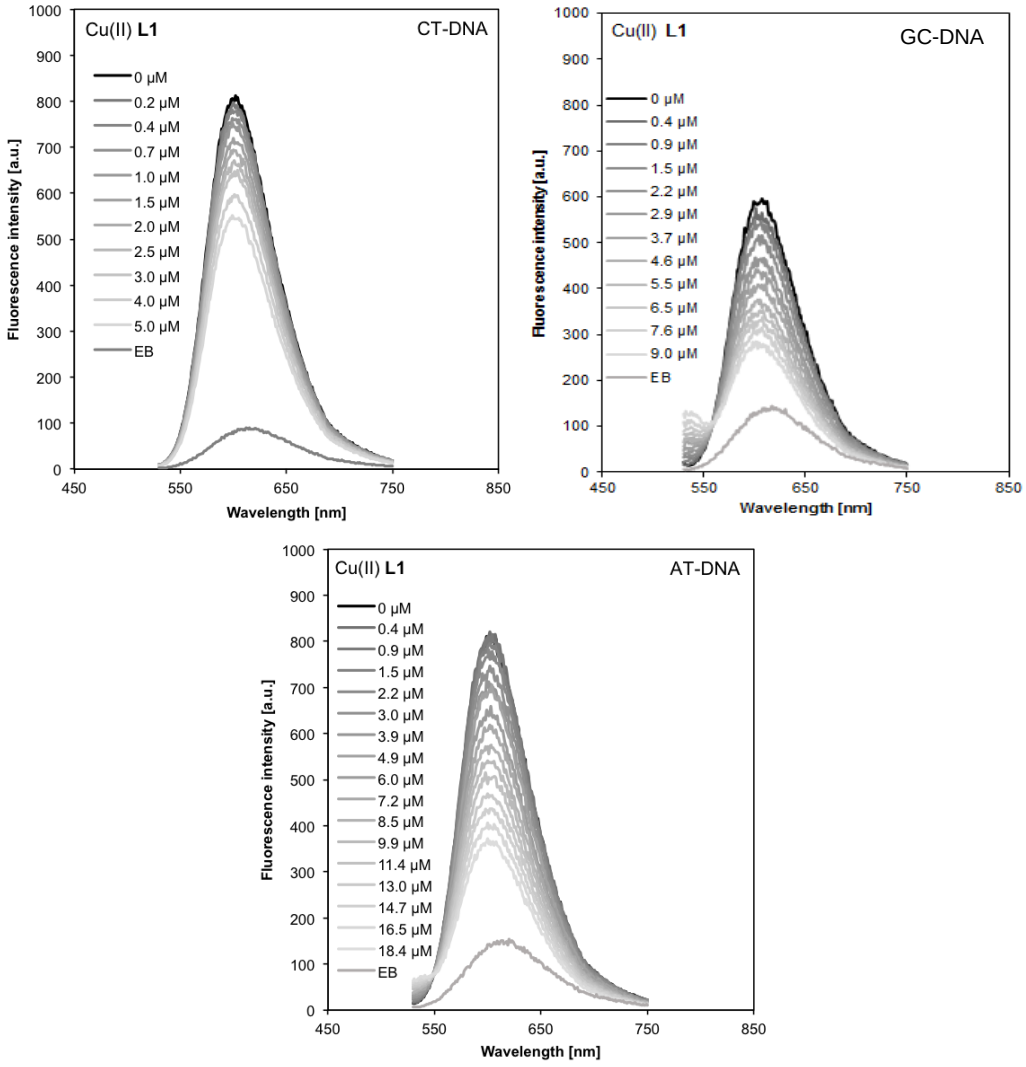

Figure S-4.1 EB displacement of CT-DNA and homopolymers poly(dG)×poly(dC) and poly(dA)×poly(dT) (20 μM DNA; 5 μM EB) in Tris-HCl buffer (10 mM, pH 7.4) by Cu(II) **L1**.

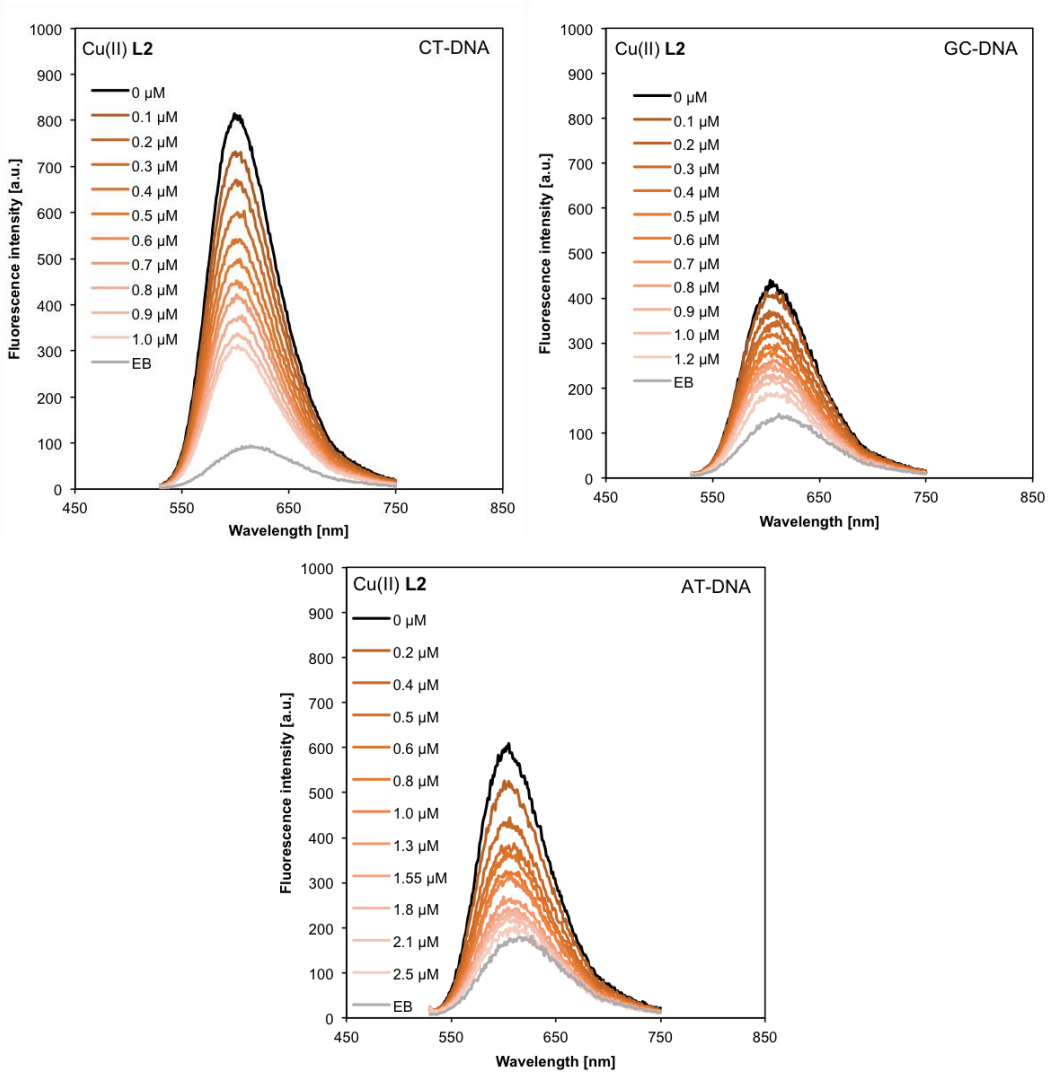

Figure S-4.2 EB displacement of CT-DNA and homopolymers poly(dG)×poly(dC) and poly(dA)×poly(dT) (20 μM DNA; 5 μM EB) in Tris-HCl buffer (10 mM, pH 7.4) by Cu(II) **L2**.

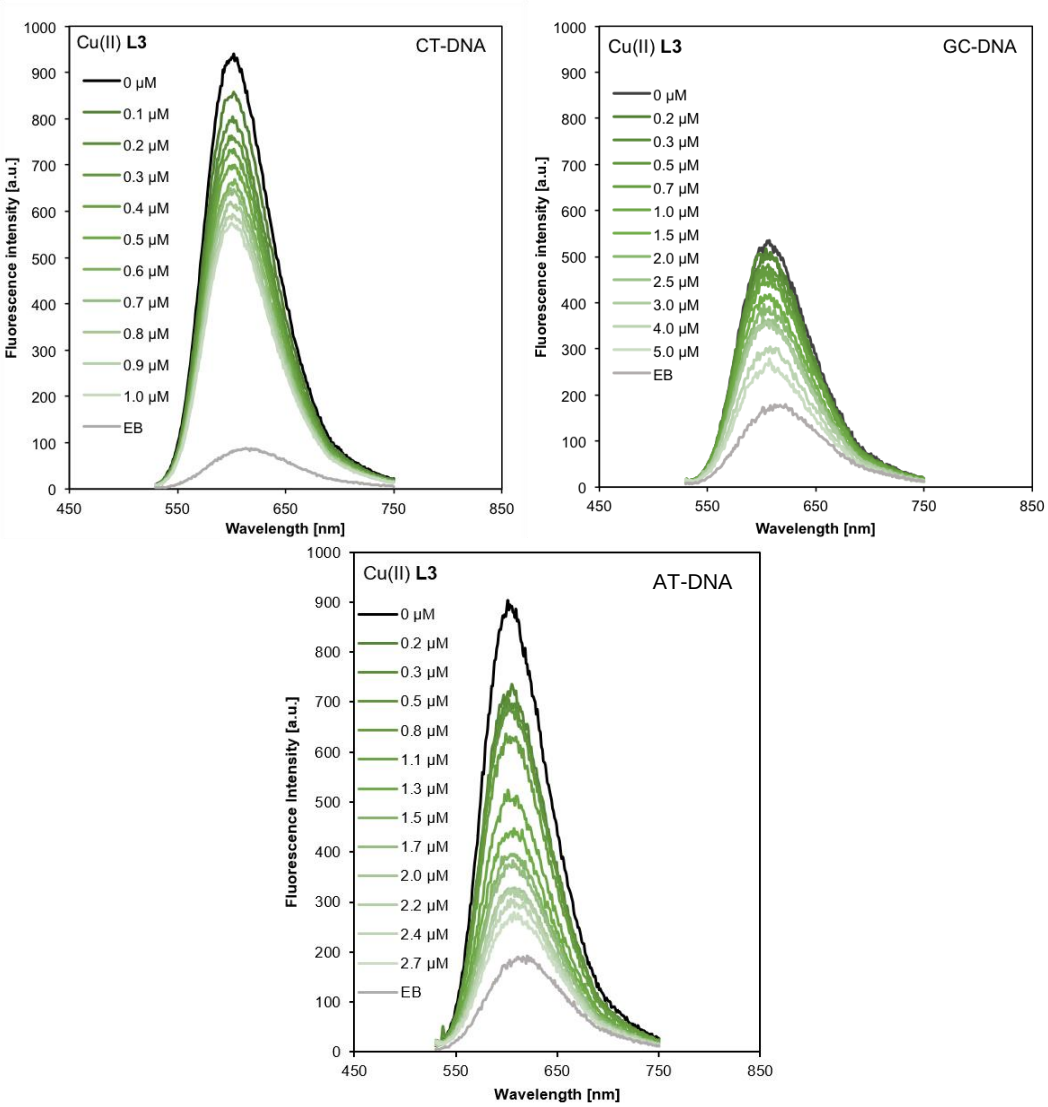

Figure S-4.3 EB displacement of CT-DNA and homopolymers poly(dG)×poly(dC) and poly(dA)×poly(dT) (20 μM DNA; 5 μM EB) in Tris-HCl buffer (10 mM, pH 7.4) by Cu(II) **L3**.

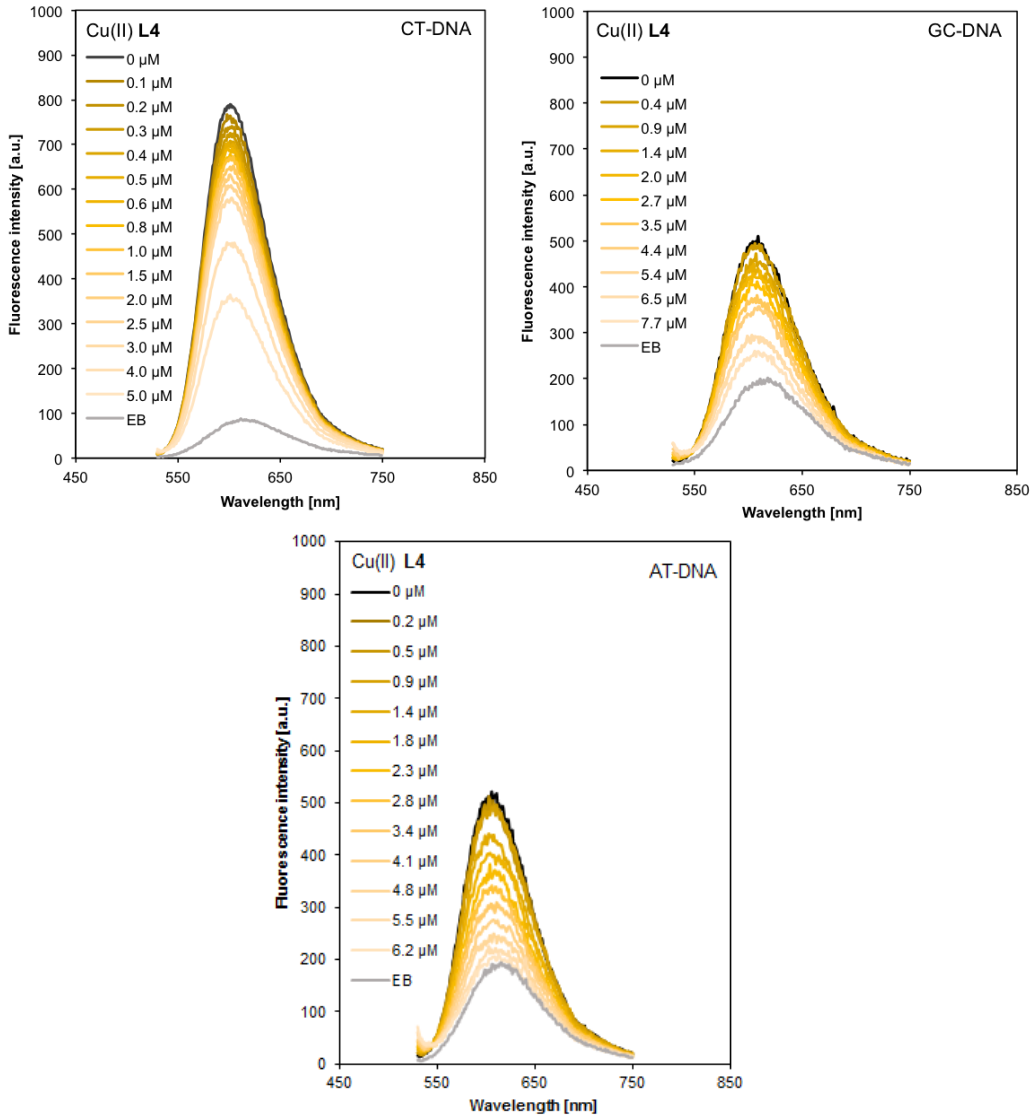

Figure S-4.4 EB displacement of CT-DNA and homopolymers poly(dG)×poly(dC) and poly(dA)×poly(dT) (20 μM DNA; 5 μM EB) in Tris-HCl buffer (10 mM, pH 7.4) by Cu(II) **L4**.

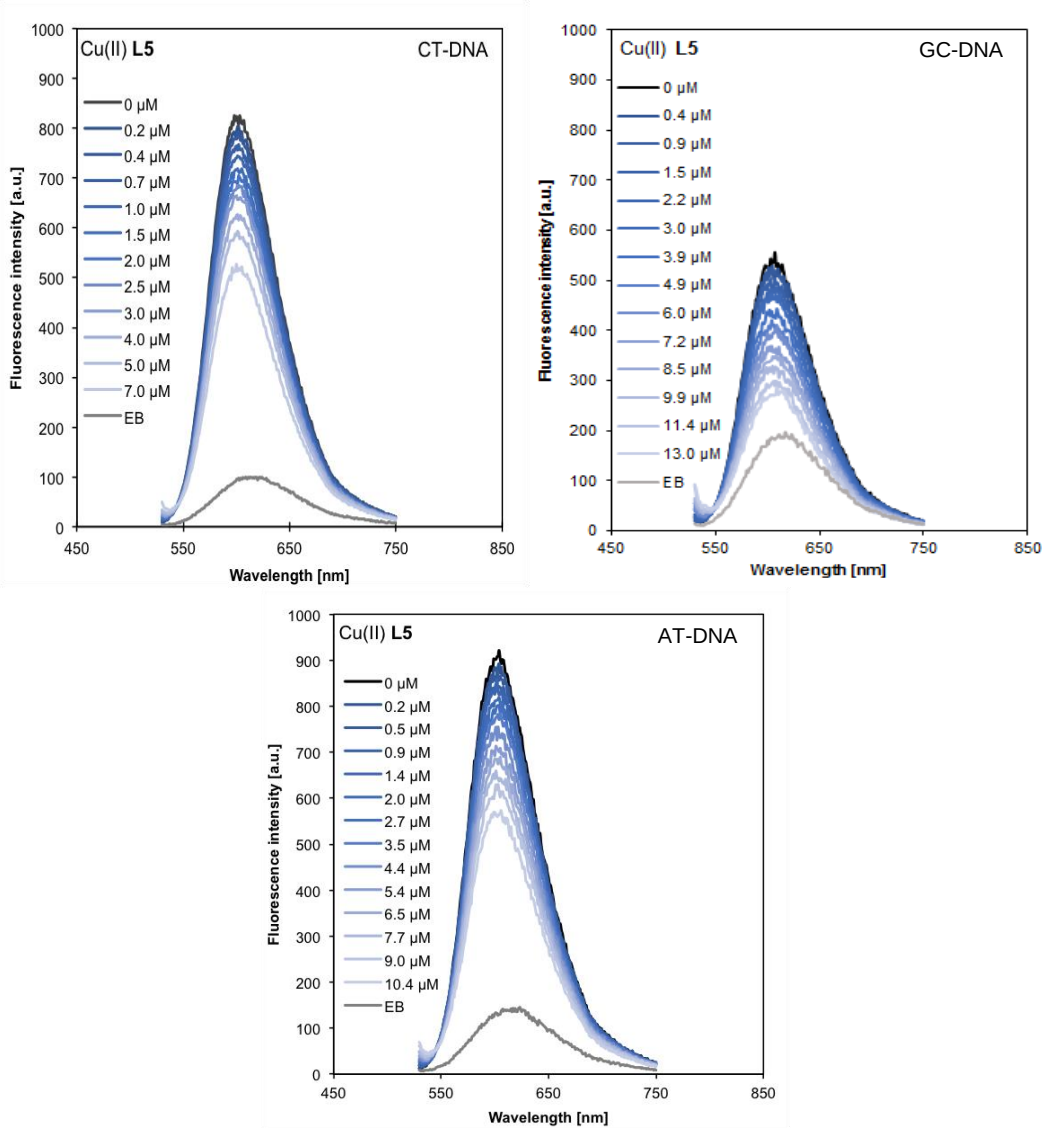

Figure S-4.5 EB displacement of CT-DNA and homopolymers poly(dG)×poly(dC) and poly(dA)×poly(dT) (20 μM DNA; 5 μM EB) in Tris-HCl buffer (10 mM, pH 7.4) by Cu(II) **L5**.

S-5 Total intensity light scattering

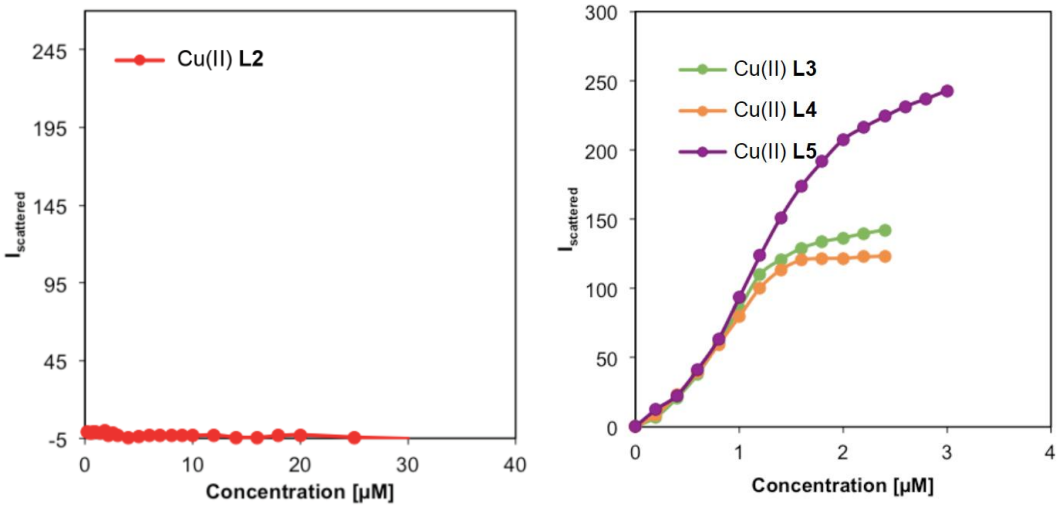

Figure S-5 Total intensity light scattering curves of 1.5 μM CT-DNA in the presence of increasing concentrations of Cu(II) **L2** (left) and Cu(II) **L3**–**L5** (right) in sodium cacodylate buffer (10 mM, pH 7.2) at 25 °C.

S-6 LD spectroscopy

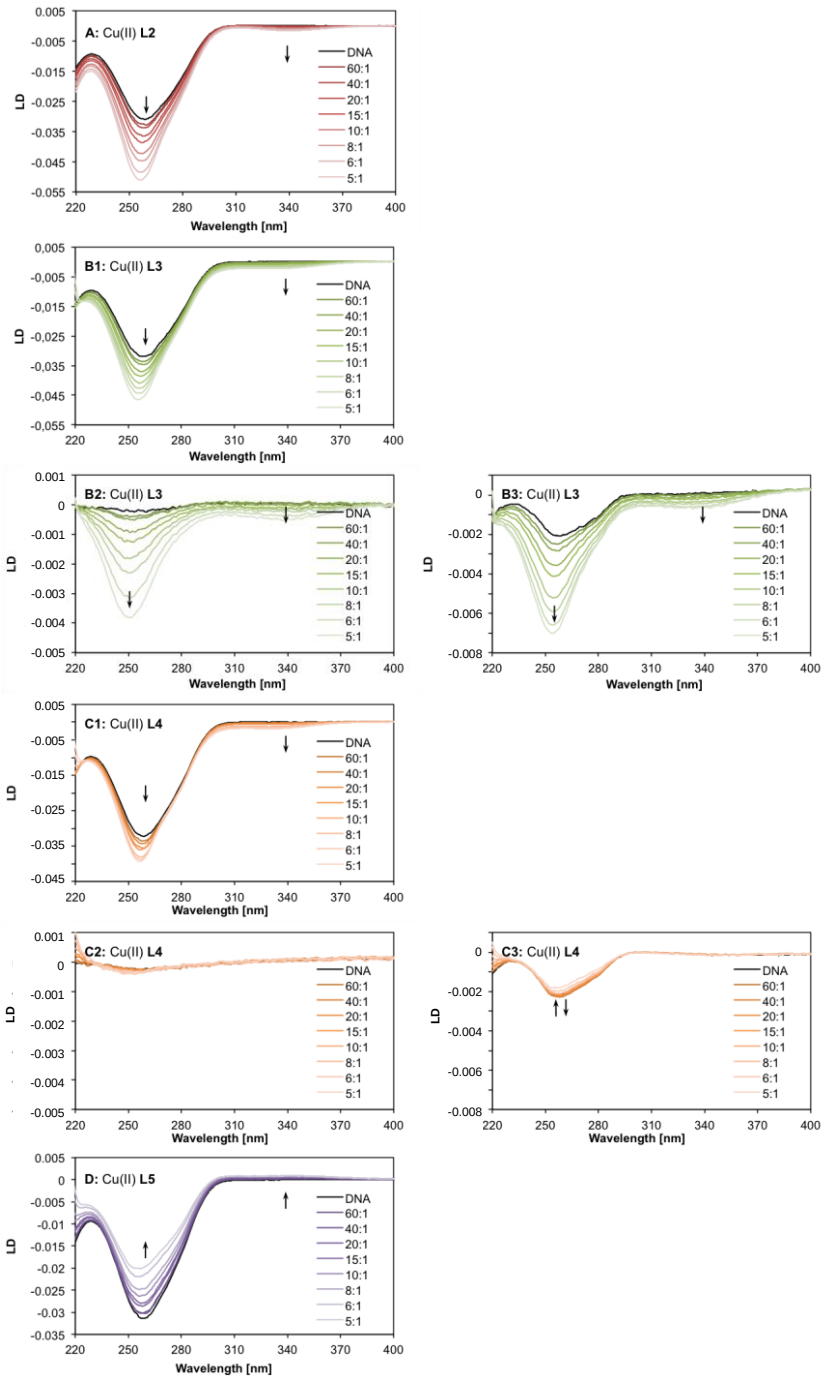

Figure S-6 LD spectra of free CT-DNA (**A**, **B1**, **C1**, **D**), poly(dG)×poly(dC) (**B2**, **C2**) and poly(dA)×poly(dT) (**B3**, **C3**), respectively (2×10^{-4} M; 10 mM Tris-HCl, pH 7.4), and in the presence of increasing concentrations of Cu(II) **L2** (**A**), Cu(II) **L3** (**B1–B3**), Cu(II) **L4** (**C1–C3**) and Cu(II) **L5** (**D**). Mixing ratios (DNA base:complex) are indicated in the figure.

S-7 Gel retardation

L2:

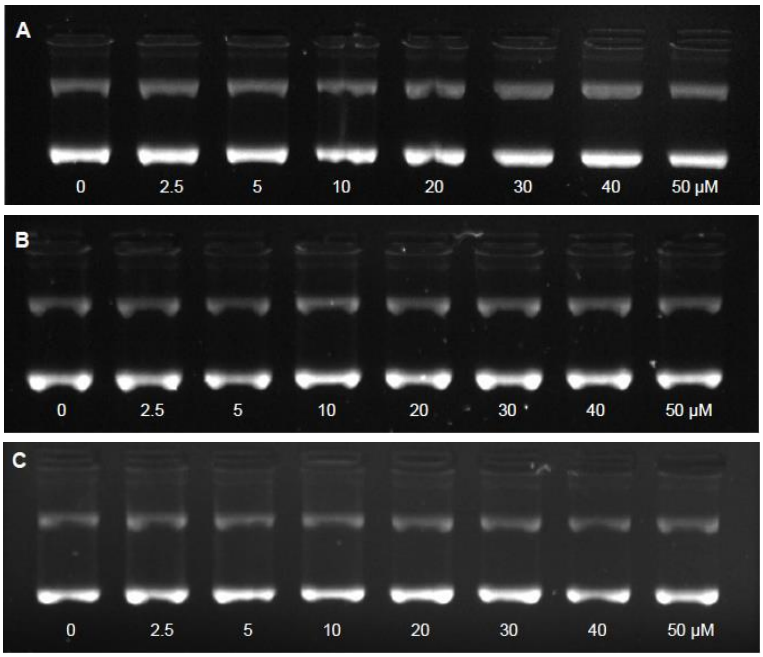

Figure S-7.1 Effect of **L2** (**A**), Zn(II) **L2** (**B**) and Cu(II) **L2** (**C**) on the migration of pBR322 plasmid DNA (0.025 µg µL^{-1}) in an agarose gel (1%) after 30 min incubation in Tris-HCl buffer (50 mM, pH 7.4) at 37 °C. For the sake of comparison the DMSO concentration was adjusted to 1% in all incubation samples.

L3:

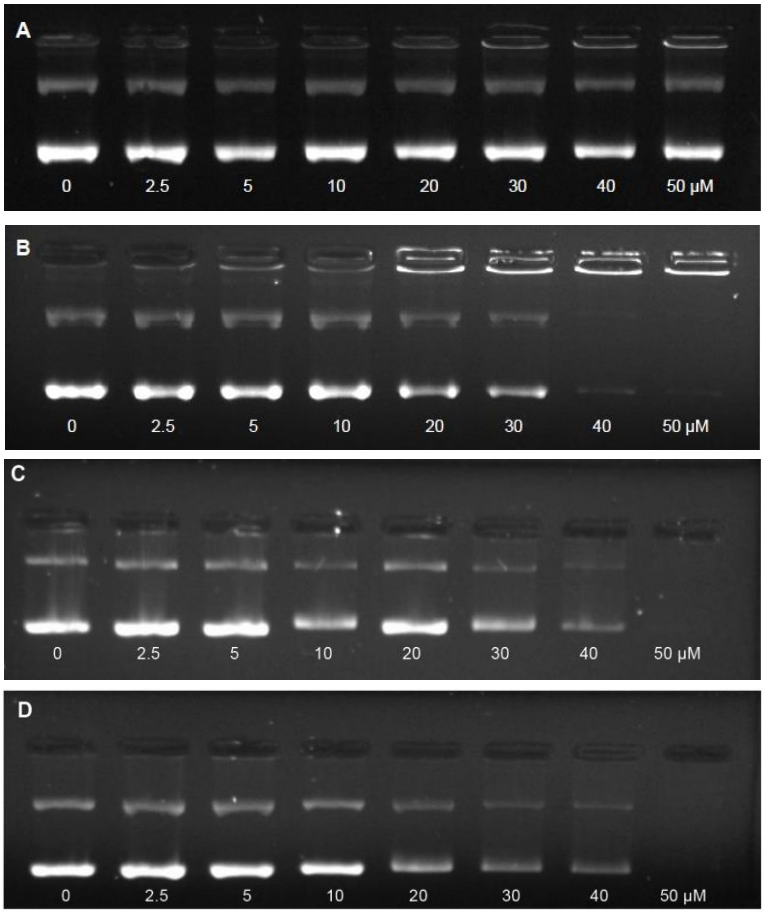

Figure S-7.2 Effect of **L3** (**A**), Zn(II) **L3** (**B**) and Cu(II) **L3** (**C**, **D**) on the migration of pBR322 plasmid DNA (0.025 μg μL^{-1}) in an agarose gel (1%) after 30 min incubation in Tris-HCl (**A**-**C**) and MOPS (**D**) buffer (50 mM, pH 7.4), respectively, at 37 °C. For the sake of comparison the DMSO concentration was adjusted to 1% in all incubation samples.

L4:

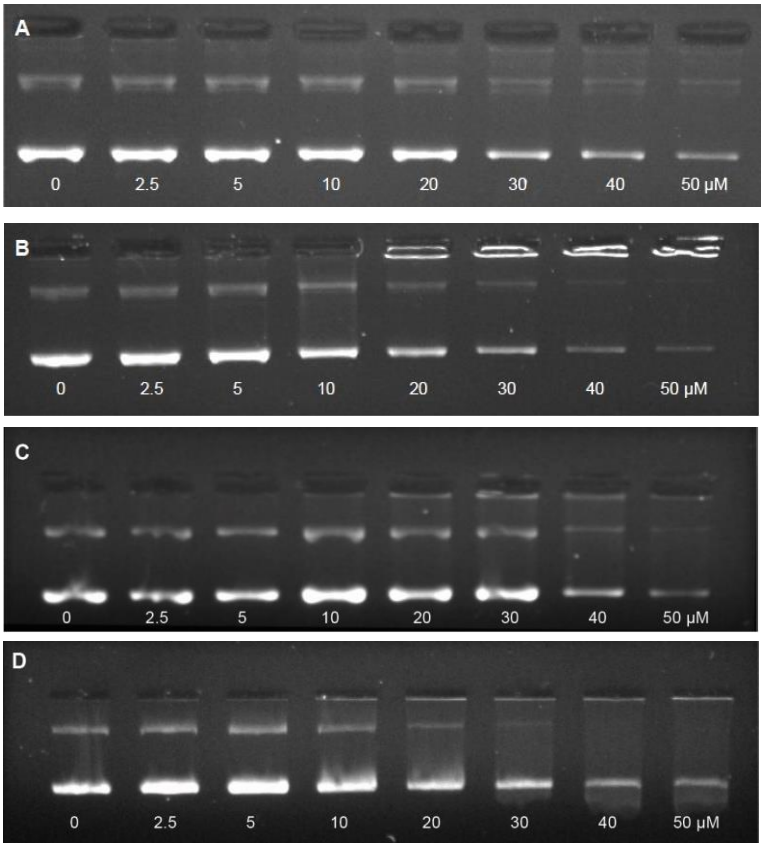

Figure S-7.3 Effect of **L4** (**A**), Zn(II) **L4** (**B**) and Cu(II) **L4** (**C**, **D**) on the migration of pBR322 plasmid DNA (0.025 μg μL^{-1}) in an agarose gel (1%) after 30 min incubation in Tris-HCl (**A**-**C**) and MOPS (**D**) buffer (50 mM, pH 7.4), respectively, at 37 °C. For the sake of comparison the DMSO concentration was adjusted to 1% in all incubation samples.

L5:

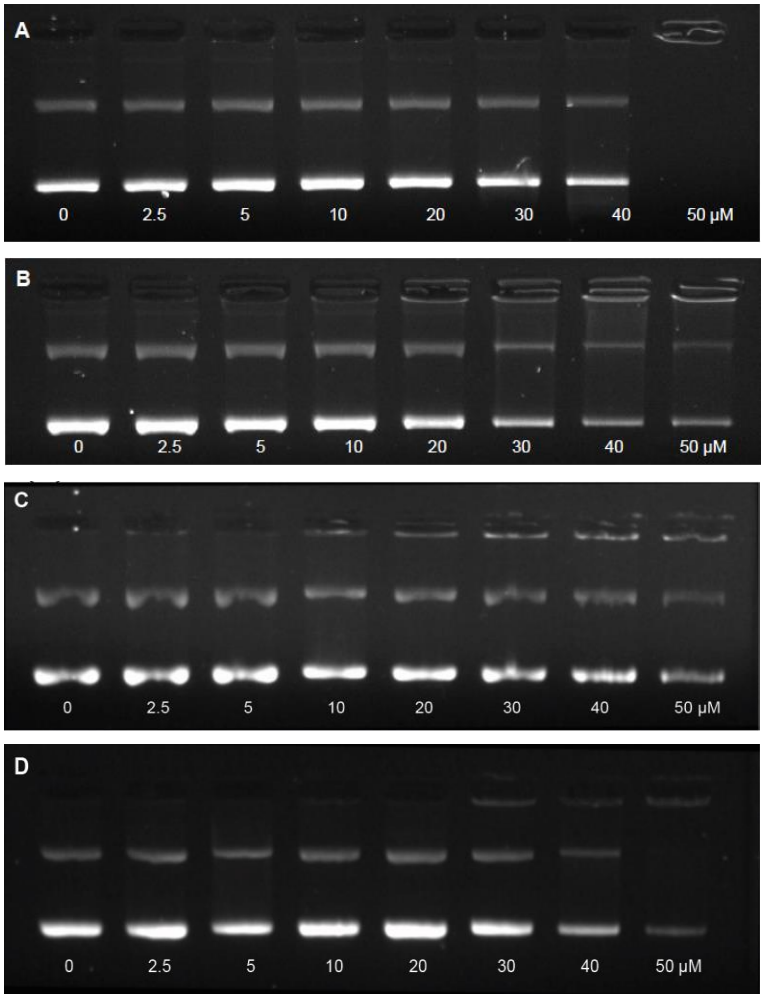

Figure S-7.4 Effect of **L5** (**A**), Zn(II) **L5** (**B**) and Cu(II) **L5** (**C**, **D**) on the migration of pBR322 plasmid DNA (0.025 µg μL^{-1}) in an agarose gel (1%) after 30 min incubation in Tris-HCl (**A**-**C**) and MOPS (**D**) buffer (50 mM, pH 7.4), respectively, at 37 °C. For the sake of comparison the DMSO concentration was adjusted to 1% in all incubation samples.

S-8 AFM imaging

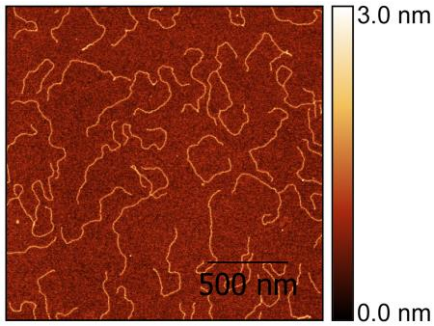

Figure S-8.1 Representative AFM image of linearized plasmid pSP73 DNA before addition of the complexes.

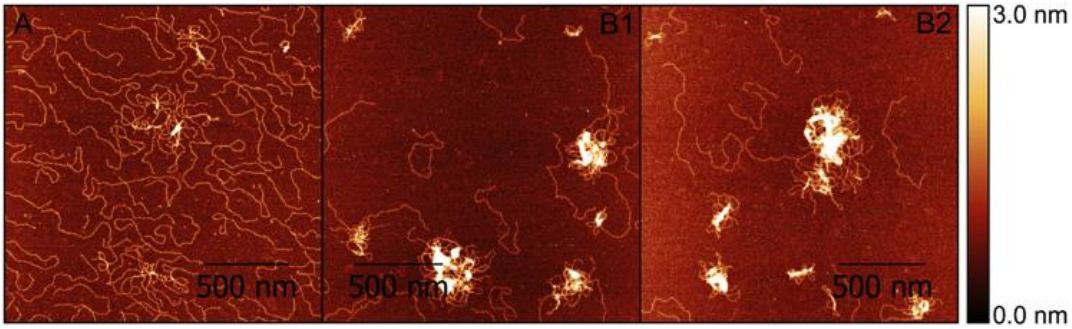

Figure S-8.2 Representative AFM images of linearized plasmid pSP73 DNA in the presence of Cu(II) **L3** at 1.56 μM (**A**) and 3.13 μM (**B1**, **B2**).

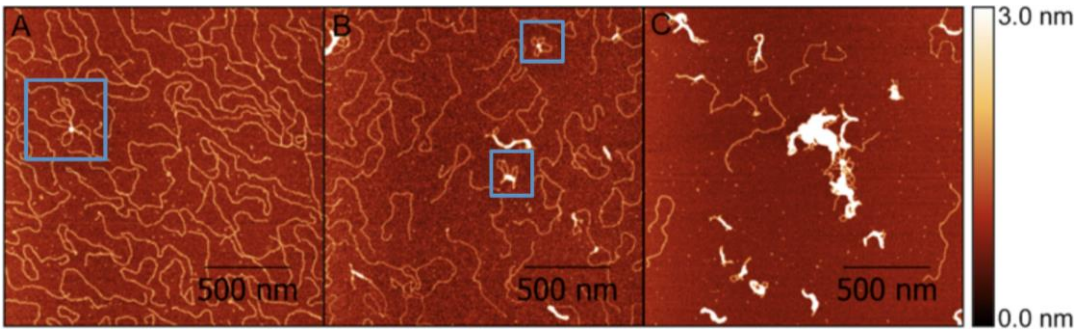

Figure S-8.3 Representative AFM images of linearized plasmid pSP73 DNA in the presence of Cu(II) **L4** at 1.56 μM (**A**), 3.13 μM (**B**), and 6.25 μM (**C**). The blue frames indicate loop structures and plectonemic coils.

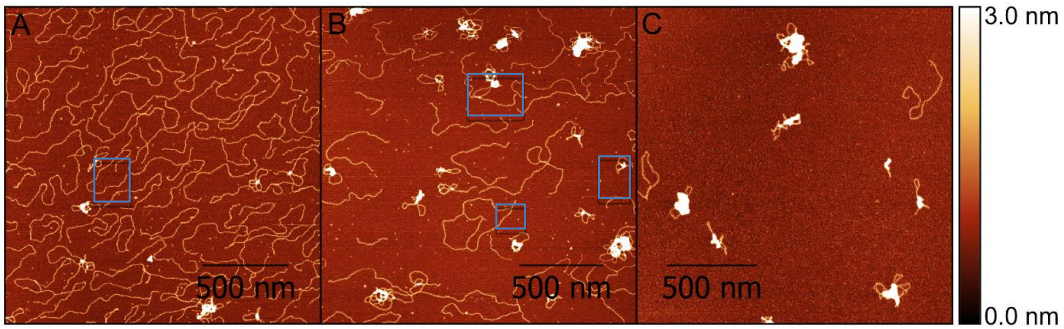

Figure S-8.4 Representative AFM images of linearized plasmid pSP73 DNA in the presence of Cu(II) **L5** at 3.13 μM (**A**), 6.25 μM (**B**), and 12.5 μM (**C**). The blue frames indicate loop structures and plectonemic coils.

S-9 PCR inhibition

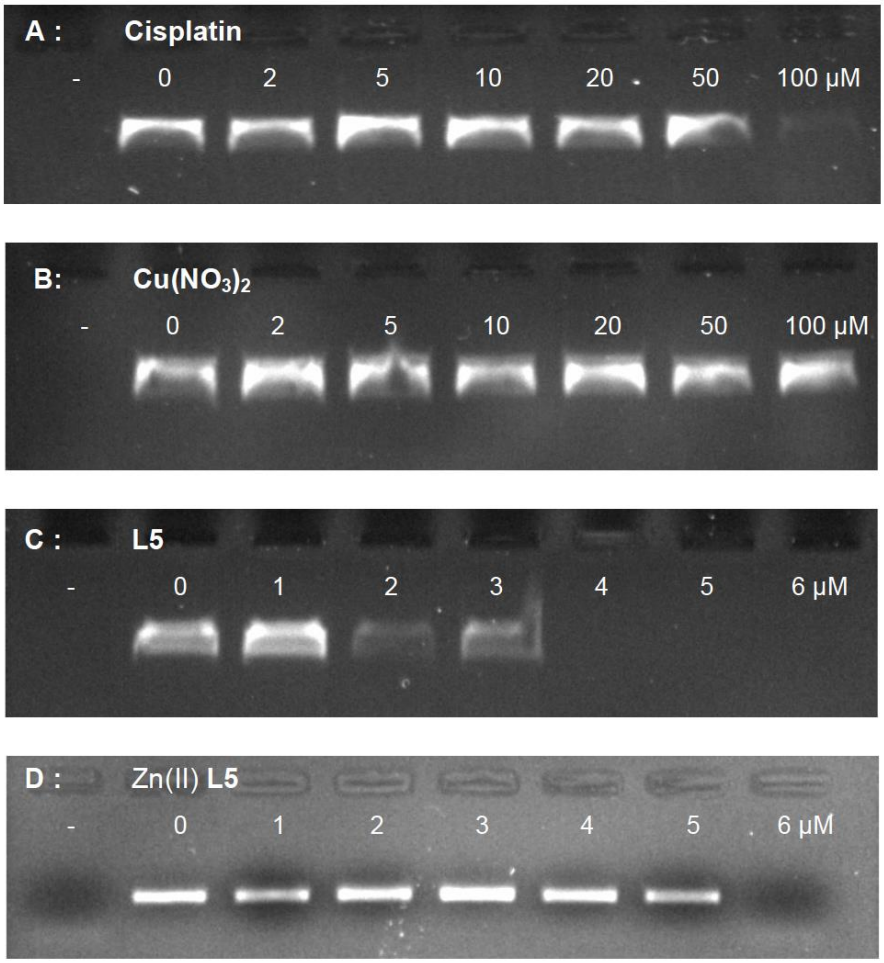

Figure S-9 Inhibition of the polymerase chain reaction (PCR) of linearized pBR322 plasmid DNA catalyzed by *Taq* polymerase in the presence of increasing concentrations of cisplatin (**A**; 0–100 µM), $Cu(NO_3)_2$ (**B**; 0–100 µM), **L5** (**C**; 0–6 µM) and Zn(II) **L5** (**D**; 0–6 µM) analyzed by agarose gel electrophoresis.

S-10 DNA transcriptional activity

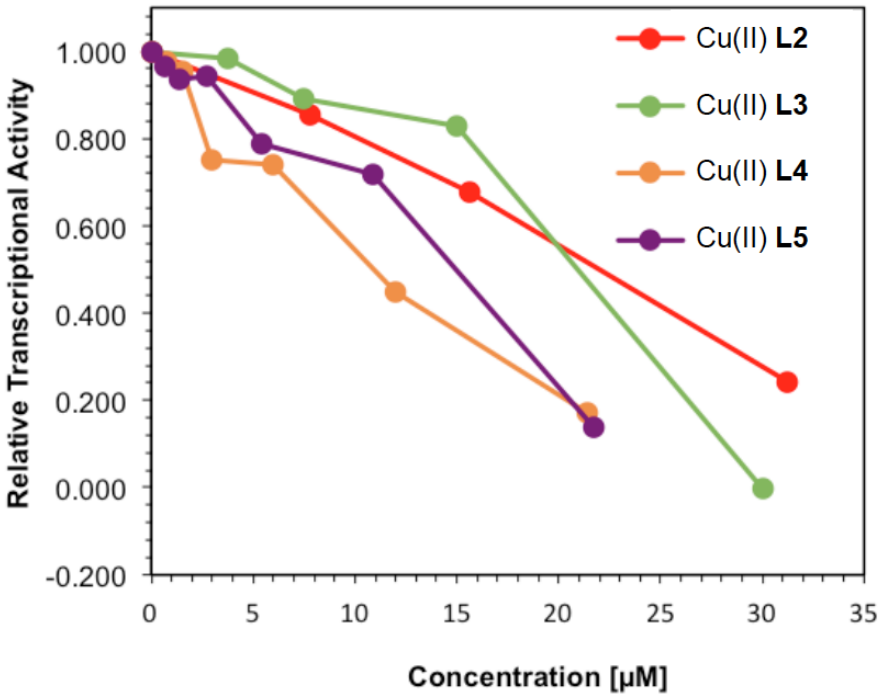

Figure S-10 The dependence of relative transcriptional activity of pBR322 plasmid DNA on the concentration of Cu(II) **L2**–**L5**. The concentration of plasmid DNA was 30 μM per nucleotide.

S-11 MTT assay

A549 cells	NHDF cells
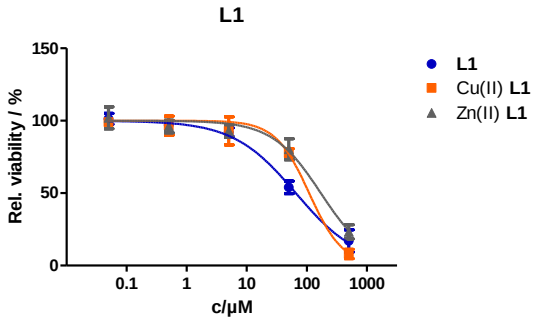	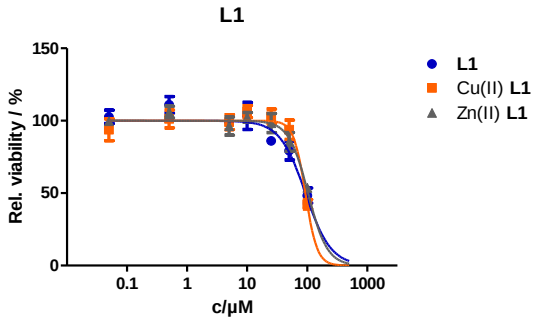
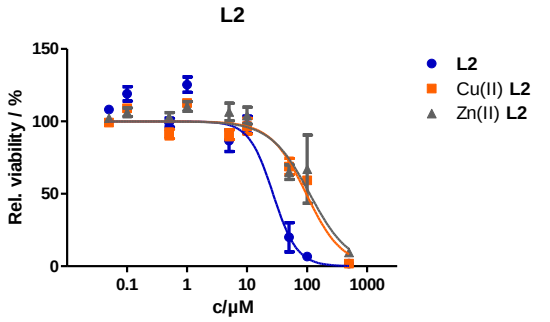	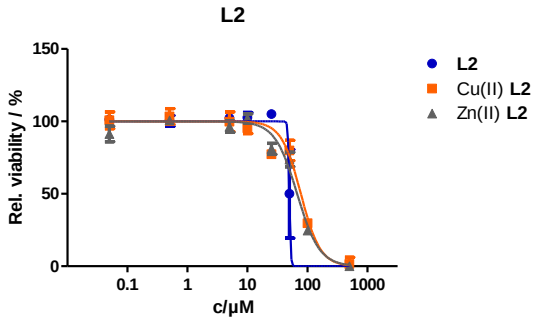
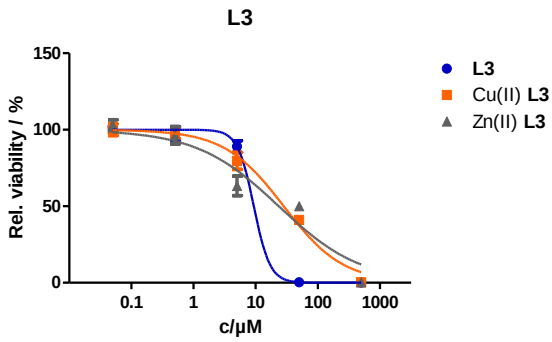	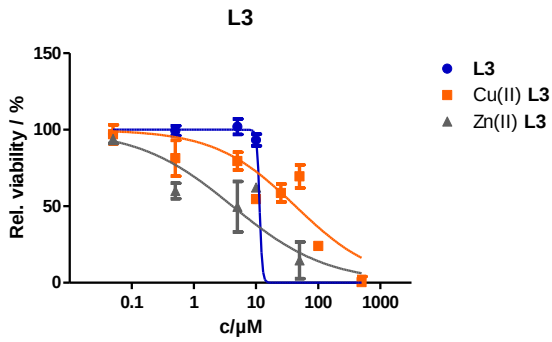
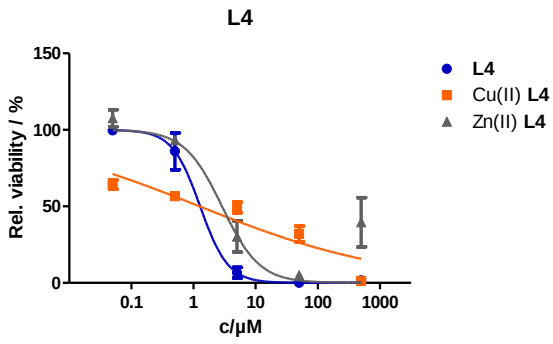	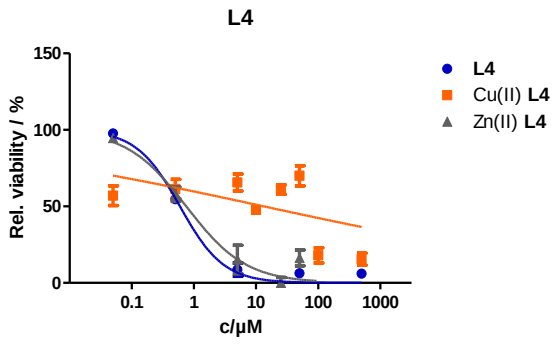

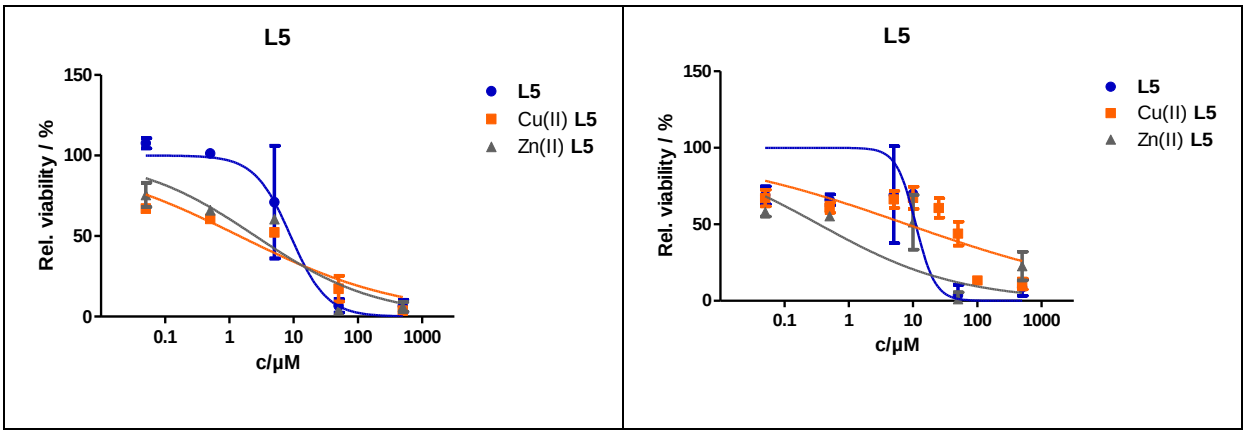

Figure S-11 Dose-response curves of A549 (left) and human dermal fibroblast (right) cells after 48 h incubation with increasing concentrations of **L1**–**L5** and their corresponding Cu(II) and Zn(II) complexes obtained by the MTT assay.

Table S-11 Complete list of IC_{50} [µM] values and 95% confidence intervals (CI, in parentheses) obtained by the MTT assay on A549 and NHDF cells for the ligands **L1**–**L5** and their Cu(II) and Zn(II) complexes compared with the reference drugs doxorubicin and cisplatin.

*The IC_{50} value for doxorubicin in NHDF cells was obtained by the trypan blue assay.[24]

	A549	**NHDF**
L1	65.6 (45.7–94.2)	93.3 (73.0–119.3)
Cu(II) **L1**	109.4 (71.3–167.7)	93.1 (79.5–109.2)
Zn(II) **L1**	171.0 (109.9–266.3)	103.3 (86.0–124.0)
L2	27.1 (18.3-40.1)	~50.0 (n/a)
Cu(II) **L2**	96.9 (77.8-120.6)	77.6 (62.9–95.7)
Zn(II) **L2**	110.5 (79.3–153.9)	67.3 (59.0–76.8)
L3	9.4 (2.6–33.6)	~ 11.4 (n/a)
Cu(II) **L3**	28.3 (20.4–39.2)	43.2 (23.5–79.3)
Zn(II) **L3**	23.6 (12.0–46.4)	4.2 (1.6–11.0)
L4	1.3 (0.8–2.0)	0.6 (0.5–0.8)
Cu(II) **L4**	1.3 (0.4–3.5)	13.4 (2.2–80.2)
Zn(II) **L4**	2.9 (1.0–8.0)	0.7 (0.5–1.2)
L5	9.0 (3.0–27.0)	11.0 (7.2–17.0)
Cu(II) **L5**	1.4 (0.6–3.5)	8.1 (3.1–21.2)
Zn(II) **L5**	2.5 (0.7–9.0)	0.3 (0.1–2.2)
Cisplatin	13.0 (n/a)[25]	94.6 (n/a)[25]
Doxorubicin	2.0 (n/a)[26]	2.5 (n/a)[24]

S-12 Flow cytometry

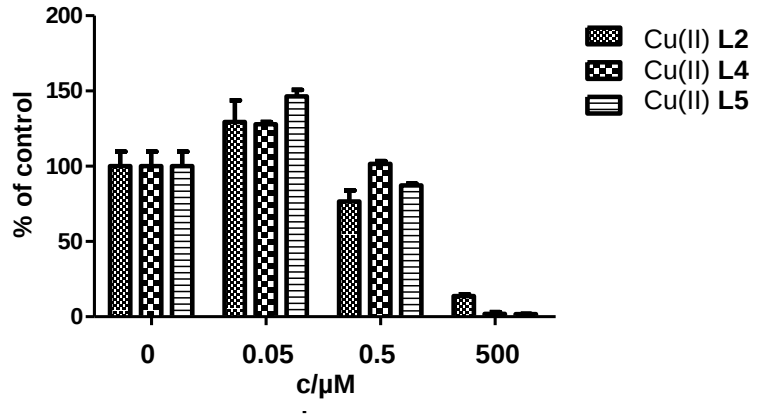

Figure S-12 Relative cell numbers of NHDF cells incubated with Cu(II) **L2**, Cu(II) **L4** and Cu(II) **L5** for 48 h at three different concentrations to determine whether low relative viability data obtained by MTT test reflects metabolic activity or cell number.

S-13 Cellular uptake

An extrapolation of the calibration curve was used to determine the copper content in untreated A549 cells. This value (1.65 ± 0.33 nmol Cu/mg protein) was subtracted from the ones obtained for the cells treated with the Cu(II) complexes to give the values of the following table.

Table S-13 Uptake of Cu(II) **L1** and Cu(II) **L4** into A549 cells measured by AAS.

Compound	Incubation time [h]	nmol Cu/mg cellular protein
Cu(II) **L1**	6	0.04 ± 0.02
Cu(II) **L1**	24	0.07 ± 0.05
Cu(II) **L4**	6	1.24 ± 0.45
Cu(II) **L4**	24	2.66 ± 0.55

S-14 Molecular Modeling

The energy minimized complexes Cu(II) **L3**-**L5** were inserted into a short DNA duplex of the below-mentioned sequence with A-DNA conformation (crystal structure PDB-ID:440D). The line indicates the intercalation site:
5'-AGGGG|CCCCT-3'
3'-TCCCC |GGGGA-5'
The sequence was chosen due to similarity to the used plasmids pBR322 and pSP73, which exhibit GGGGC motifs three and two times, respectively.

Hambley *et al.*[27] have suggested an insertion of the AQ moiety of an AQ-substituted cyclam Cu(II) complex into the DNA double helix, whereby the complex was in either a parallel or perpendicular position. The former case was not possible here due to a shorter linker length ($(CH_2)_{2/3}$ vs. CH_2) between the AQ and the macrocycle.

The insertion of the Cu(II) complexes was performed from the major as well as from the minor groove (Figures S-14.1 to S-14.4). The resulting metal complex DNA adducts were solvated and the conformational energy was calculated using GROMACS simulation package 5.0.2.[18] Within the accuracy of the used force field no significant energy differences between the different binding modes were observed. Further ligand conformations for Cu(II) **L4** and Cu(II) **L5** were generated using AutoDockTools.[15] Within these conformations one conformation was found that shows potential for bisintercalation into the minor groove of the used A-DNA structure (Figure 5 and Figure S-14.5). This is nearly impossible for B-DNA due to steric reasons (Figure S-14.6).
As can be seen from Figure 6 and Figure S-14.5, the AQ moiety is not perfectly planar (averaged deviation of the O atoms 0.29 Å with respect to the ring plane), which is at first surprising. However, also the molecular structure of e.g. 1,4-diethoxy-9,10-anthraquinone in the solid state exhibited such a deviation (CCDC 1008606, deviation of 0.24 Å).[28]

Figure S-14.1 Cu(II) **L3** in the minor groove, A-DNA.

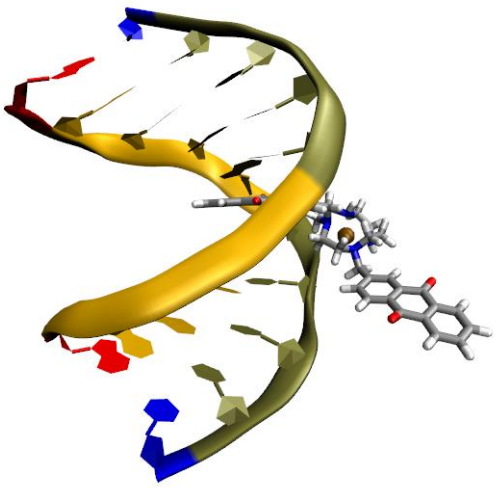

Figure S-14.2 Cu(II) **L3** in the major groove, A-DNA.

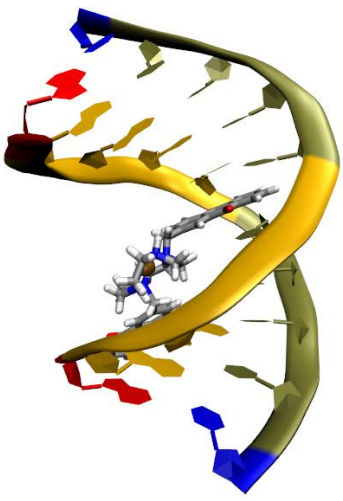

Figure S-14.3 Cu(II) **L4** in the minor groove, A-DNA.

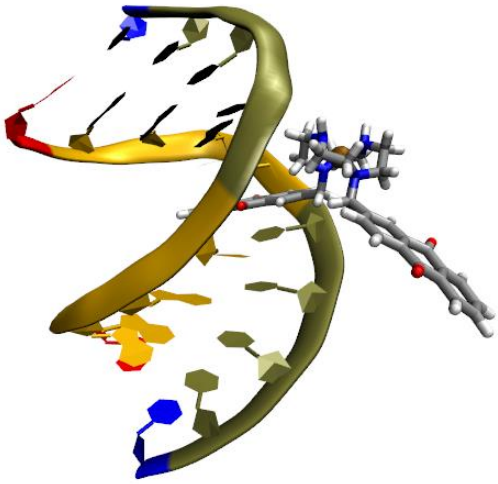

Figure S-14.4 Cu(II) **L4** in the major groove, A-DNA.

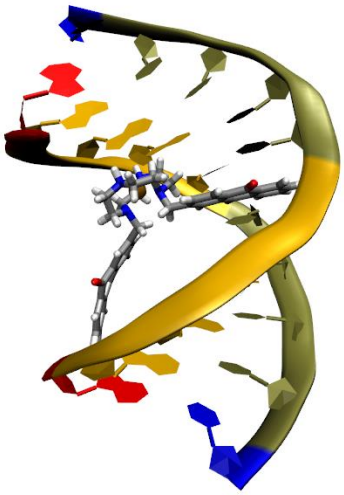

Figure S-14.5 Bisintercalation of Cu(II) **L5** in the minor groove, A-DNA.

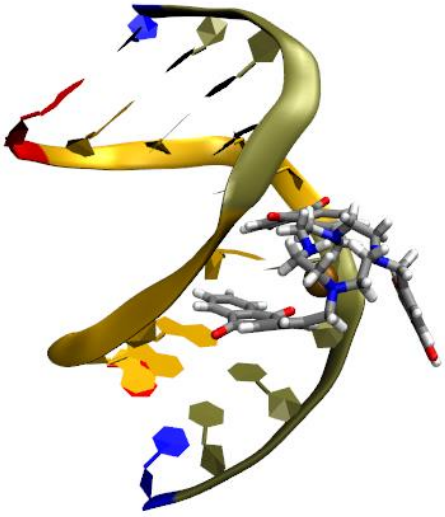

Figure S-14.6 Bisintercalation of Cu(II) **L4** in the minor groove, B-DNA.

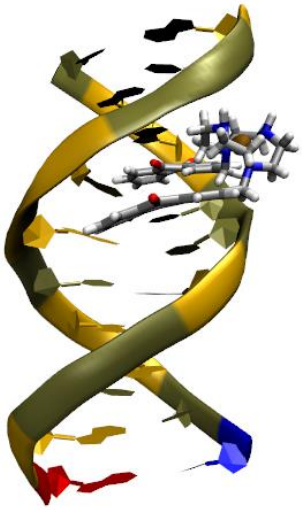

Figure S-14.7 Energy-minimized Cu(II) **L4** showing the distance of the AQ moieties.

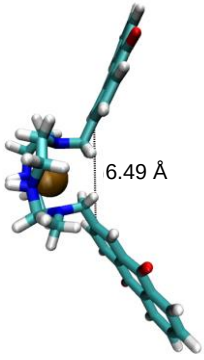

References

(1) Furuta, T.; Torigai, H.; Sugimoto, M.; Iwamura, M. Photochemical Properties of New Photolabile cAMP Derivatives in a Physiological Saline Solution. *J. Org. Chem.* **1995**, *60*, 3953–3956.

(2) Tucker, J. H. R.; Shionoya, M.; Koike, T.; Kimura, E. A Zinc(II)–Cyclen Complex Attached to an Anthraquinone Moiety That Acts as a Redox-Active Nucleobase Receptor in Aqueous Solution. *Bull. Chem. Soc. Jpn.* **1995**, *68*, 2465–2469.

(3) Bellouard, F.; Chuburu, F.; Kervarec, N.; Toupet, L.; Triki, S.; Le Mest, Y.; Handel, H. Cis-Diprotected Cyclams and Cyclens: A New Route to Symmetrically or Asymmetrically 1,4-Disubstituted Tetraazamacrocycles and to Asymmetrically Tetrasubstituted Derivatives. *J. Chem. Soc., Perkin Trans. 1* **1999**, 3499–3505.

(4) De León-Rodríguez, L. M.; Kovacs, Z.; Esqueda-Oliva, A. C.; Miranda-Olvera, A. D. Highly Regioselective N-Trans Symmetrical Diprotection of Cyclen. *Tetrahedron Lett.* **2006**, *47*, 6937–6940.

(5) Dolomanov, O. V.; Bourhis, L. J.; Gildea, R. J.; Howard, J. A. K.; Puschmann, H. *OLEX2* : A Complete Structure Solution, Refinement and Analysis Program. *J. Appl. Crystallogr.* **2009**, *42*, 339–341.

(6) Bourhis, L. J.; Dolomanov, O. V.; Gildea, R. J.; Howard, J. A. K.; Puschmann, H. The Anatomy of a Comprehensive Constrained, Restrained Refinement Program for the Modern Computing Environment – *Olex2* Dissected. *Acta Crystallogr., Sect. A: Found. Adv.* **2015**, *71*, 59–75.

(7) Sheldrick, G. M. A Short History of *SHELX*. *Acta Crystallogr., Sect. A: Found. Crystallogr.* **2008**, *64*, 112–122.

(8) Rodger, A.; Nordén, B. *Circular Dichroism and Linear Dichroism*; Oxford University Press, **1997**.

(9) Rodger, A. Linear Dichroism. *Methods Enzymol.* **1993**, *226*, 232–258.

(10) Vijayanathan, V.; Thomas, T.; Shirahata, A.; Thomas, T. J. DNA Condensation by Polyamines: A Laser Light Scattering Study of Structural Effects. *Biochemistry* **2001**, *40*, 13644–13651.

(11) Luckel, F.; Kubo, K.; Tsumoto, K.; Yoshikawa, K. Enhancement and Inhibition of DNA Transcriptional Activity by Spermine: A Marked Difference between Linear and Circular Templates. *FEBS Lett.* **2005**, *579*, 5119–5122.

(12) Gao, Y.-G.; Robinson, H.; Wang, A. H.-J. High-Resolution A-DNA Crystal Structures of d(AGGGGCCCCT). An A-DNA Model of poly(dG)·poly(dC). *Eur. J. Biochem.* **1999**, *261*, 413–420.

(13) Marvin 16.8.1, ChemAxon. **2016**.

(14) Hanwell, M. D.; Curtis, D. E.; Lonie, D. C.; Vandermeersch, T.; Zurek, E.; Hutchison, G. R. Avogadro: An Advanced Semantic Chemical Editor, Visualization, and Analysis Platform. *J. Cheminform.* **2012**, *4*, 17.

(15) Morris, G. M.; Huey, R.; Lindstrom, W.; Sanner, M. F.; Belew, R. K.; Goodsell, D. S.; Olson, A. J. AutoDock4 and AutoDockTools4: Automated Docking with Selective Receptor Flexibility. *J. Comput. Chem.* **2009**, *30*, 2785–2791.

(16) The PyMOL Molecular Graphics System. Schrödinger LLC.

(17) Jorgensen, W. L.; Chandrasekhar, J.; Madura, J. D.; Impey, R. W.; Klein, M. L. Comparison of Simple Potential Functions for Simulating Liquid Water. *J. Chem. Phys.* **1983**, *79*, 926–935.

(18) Van Der Spoel, D.; Lindahl, E.; Hess, B.; Groenhof, G.; Mark, A. E.; Berendsen, H. J. C. GROMACS: Fast, Flexible, and Free. *J. Comput. Chem.* **2005**, *26*, 1701–1718.

(19) Cornell, W. D.; Cieplak, P.; Bayly, C. I.; Gould, I. R.; Merz, K. M.; Ferguson, D. M.; Spellmeyer, D. C.; Fox, T.; Caldwell, J. W.; Kollman, P. A. A Second Generation Force Field for the Simulation of Proteins, Nucleic Acids, and Organic Molecules. *J. Am. Chem. Soc.* **1995**, *117*, 5179–5197.

(20) Case, D. A.; Betz, R. M.; Cerutti, D. S.; Cheatham, III, T.E.; Darden, T. A.; Duke, R. E.; Giese, T. J.; Gohlke, H.; Goetz, A. W.; Homeyer, N.; Izadi, S.; Janowski, P.; Kaus, J.; Kovalenko, A.; Lee, T. S.; LeGrand, S.; Li, P.; Lin, C.; Luchko, T.; Luo, R.; Madej, B.; Mermelstein, D.; Merz, K. M.; Monard, G.; Nguyen, H.; Nguyen, H. T.; Omelyan, I.; Onufriev, A.; Roe, D. R.; Roitberg, A.; Sagui, C.; Simmerling, C. L.; Botello-Smith, W. M.; Swails, J.; Walker, R. C.; Wang, J.; Wolf, R. M.; Wu, X.; Xiao, L.; Kollman, P. A. Amber 2016. University of California, San Francisco **2016**.

(21) Sousa da Silva, A. W.; Vranken, W. F. ACPYPE - AnteChamber PYthon Parser interfacE. *BMC Res. Notes* **2012**, *5*, 367.

(22) Lee, M.; Rhodes, A. L.; Wyatt, M. D.; Forrow, S.; Hartley, J. A. GC Base Sequence Recognition by Oligo(imidazolecarboxamide) and C-Terminus-Modified Analogues of Distamycin Deduced from Circular Dichroism, Proton Nuclear Magnetic Resonance, and Methidiumpropylethylenediaminetetraacetate-Iron(II) Footprinting Studies. *Biochemistry* **1993**, *32*, 4237–4245.

(23) Baguley, B. C.; Falkenhaug, E. M. The Interaction of Ethidium with Synthetic Double-Stranded

Polynucleotides at Low Ionic Strength. *Nucleic Acids Res.* **1978**, *5*, 161–171.
(24) Tiago, M.; Mendes de Oliveira, E.; Abdo Brohem, C.; Comune Pennacchi, P.; Duarte Paes, R.; Brandão Haga, R..; Campa, A.; Berlanga de Moraes Barros, S.; Smalley, K. S.; Stuchi Maria-Engler, S. Fibroblasts Protect Melanoma Cells from the Cytotoxic Effects of Doxorubicin. *Tissue Eng., Part A* **2014**, *20*, 2412–2421.
(25) Jayakumar, S.; Mahendiran, D.; Viswanathan, V.; Velmurugan, D.; Kalilur Rahiman, A. Heteroscorpionate-Based Heteroleptic Copper(II) Complexes: Antioxidant, Molecular Docking and in Vitro Cytotoxicity Studies. *Appl. Organomet. Chem.* **2017**, *31*, e3809.
(26) Senwar, K. R.; Sharma, P.; Reddy, T. S.; Jeengar, M. K.; Nayak, V. L.; Naidu, V. G. M.; Kamal, A.; Shankaraiah, N. Spirooxindole-Derived Morpholine-Fused-1,2,3-Triazoles: Design, Synthesis, Cytotoxicity and Apoptosis Inducing Studies. *Eur. J. Med. Chem.* **2015**, *102*, 413–424.
(27) Ellis, L. T.; Perkins, D. F.; Turner, P.; Hambley, T. W. The Preparation and Characterisation of Cyclam/anthraquinone Macrocyle/Intercalator Complexes and Their Interactions with DNA. *Dalton Trans.* **2003**, 2728–2736.
(28) Kitamura, C.; Li, S.; Takehara, M.; Inoue, Y.; Ono, K.; Kawase, T. Crystal Structure of 1,4-Diethoxy-9,10-Anthraquinone. *Acta Crystallogr., Sect. E: Crystallogr. Commun.* **2015**, *71*, o504–o505.